

Connect the Dots: Knowledge Graph–Guided Crawler Attack on Retrieval-Augmented Generation Systems

Mengyu Yao¹, Ziqi Zhang², Ning Luo³, Shaofei Li¹, Yifeng Cai¹, Xiangqun Chen¹, Yao Guo¹ and Ding Li¹

¹*MOE Key Lab of HCST (PKU), School of Computer Science, Peking University*

²*Department of Computer Science, University of Illinois Urbana-Champaign*

³*Department of Electrical and Computer Engineering, University of Illinois Urbana-Champaign*

Abstract

Stealing attacks pose a persistent threat to the intellectual property of deployed machine-learning systems. Retrieval-augmented generation (RAG) intensifies this risk by extending the attack surface beyond model weights to knowledge base that often contains IP-bearing assets such as proprietary runbooks, curated domain collections, or licensed documents. Recent work shows that multi-turn questioning can gradually steal corpus content from RAG systems, yet existing attacks are largely heuristic and often plateau early. We address this gap by formulating RAG knowledge-base stealing as an adaptive stochastic coverage problem (ASCP), where each query is a stochastic action and the attacker’s goal is to maximize the conditional expected marginal gain (CMG) in corpus coverage under a query budget. Bridging ASCP to real-world black-box RAG knowledge-base stealing raises three challenges: CMG is unobservable, the natural-language action space is intractably large, and feasibility constraints require stealthy queries that remain effective under diverse architectures. We introduce RAGCRAWLER, a knowledge graph-guided attacker that maintains a global attacker-side state to estimate coverage gains, schedule high-value semantic anchors, and generate non-redundant natural queries. Across four corpora and four generators with BGE retriever, RAGCRAWLER achieves 66.8% average coverage (up to 84.4%) within 1,000 queries, improving coverage by 44.90% relative to the strongest baseline. It also reduces the queries needed to reach 70% coverage by at least 4.03 \times on average and enables surrogate reconstruction with answer similarity up to 0.699. Our attack is also scalable to retriever switching and newer RAG techniques like query rewriting and multi-query retrieval. These results highlight urgent needs to protect RAG knowledge assets.

1 Introduction

Intellectual property (IP) theft remains a central concern across the AI service landscape. A large body of work on

model-stealing attacks and defenses [15, 20, 21, 30, 33, 34, 43, 50, 60, 63, 64, 68, 70, 75, 79, 84] underscores the urgency of protecting proprietary AI assets and preventing information theft. As modern AI service architectures grow increasingly complex, the IP attack surface extends beyond the model itself, requiring immediate investigation and comprehensive defense strategies.

Retrieval-Augmented Generation (RAG), now a ubiquitous architecture grounded in proprietary data, extends the attack surface to the retrieval corpus that sits on the path of every response. RAG couples a generator with a retriever over a document collection, using retrieved documents to improve factuality and domain adaptation [35, 40]. In enterprise and vertical deployments, the corpus often contains IP-bearing assets (e.g., proprietary runbooks and policies, curated domain data, and licensed materials) whose acquisition and maintenance are costly [6, 52, 80]. Because each response is grounded in retrieved documents, the public chat or API interface [27] becomes an attack surface: an attacker can progressively steal more of the underlying corpus using curated queries. Stealing a sufficiently large portion of the corpus can be enough to replicate the service: an attacker can pair the stolen corpus with an off-the-shelf LLM to build a substitute RAG assistant that approximates the victim’s behavior without access to the original deployment [76].

Recent studies highlight that *knowledge-base stealing* poses an important and growing threat to deployed RAG systems, with direct copyright, licensing, and privacy implications for IP-bearing corpora [32, 66, 76, 85]. Attackers can elicit verbatim or near-verbatim spans from RAG outputs [66, 85], and sustained multi-turn interaction can cumulatively expand the portion of a hidden corpus that becomes exposed [32, 76]. However, existing attacks typically generate prompts by locally reacting to the most recent response, either continuing the thread or pivoting on extracted keywords [32, 76]. Such heuristics often drift off-topic (left panel of Fig. 1 (a)) or revisit already-exposed regions (middle panel of Fig. 1 (a)), wasting query budget and plateauing early, leaving much of the corpus unexplored (Fig. 1 (b)). Moreover,

while prior empirical studies demonstrate the knowledge-base theft, theoretical grounding and provable guarantees for coverage-maximizing attacks remain unknown. This motivates a critical question: *can the adversary steal the data more efficiently, and where is the limit?*

To address this question, we identify the fundamental gap in existing work: *lack of a principled objective to maximize global corpus coverage*. Without such an objective, query selection is driven by local reactions to the latest response, providing no globally consistent criterion to avoid redundancy and systematically expand coverage across turns. An effective knowledge-base stealing strategy should instead exploit the *global state* accumulated over the entire interaction history and choose each query by its *expected marginal contribution* to previously unseen corpus content.

We formalize this global objective by casting RAG knowledge-base stealing as *RAG Crawling*, an instance of the **Adaptive Stochastic Coverage Problem (ASCP)** [26, 58, 78]. In our reduction, each query is an action that stochastically reveals a subset of hidden documents through retrieval, and the attacker aims to maximize the expected coverage of unique corpus items under a fixed query budget. ASCP provides an adaptive-greedy benchmark that selects the query with the largest *conditional expected marginal gain (CMG)* at each step. We further prove that *RAG Crawling* satisfies adaptive monotonicity and adaptive submodularity; thus, under the same budget of B queries, the CMG-based adaptive greedy attack is provably near-optimal, achieving a $(1 - 1/e)$ -approximation to the expected corpus coverage attainable by an optimal adaptive attacker.

However, implementing this theory into a practical black-box attack faces three key instantiation challenges. **① CMG is unobservable:** the attacker cannot directly measure the coverage increment induced by a query and its retrieval outcome without corpus access, so the true CMG cannot be exactly computed. **② The action space is intractable:** the query space Q is effectively unbounded (any natural-language string), making it infeasible to exhaustively search for the CMG-maximizing query without additional structure. **③ Real-world feasibility constraints are strict:** queries must remain natural and innocuous to avoid detection or refusal, and high-gain intents must be expressed in policy-compliant surface forms that remain stable under query rewriting and multi-query retrieval.

To solve these challenges, we introduce RAGCRAWLER, a novel attack framework consisting of three stages: knowledge graph construction, strategy scheduling, and query generation, that together overcome the above challenges. RAGCRAWLER maintains an attacker-side knowledge graph (KG) that provides a global summary of acquired information and supports planning. With this global state, RAGCRAWLER first uses KG growth in KG construction phase to estimate coverage gain and CMG. RAGCRAWLER next prunes the action space by selecting high-value semantic anchors in strategy scheduling

phase. These semantic anchors are determined based on historical gains and the structural exploration of the KG. During the query generation phase, RAGCRAWLER enforces real-world feasibility by turning top-ranked anchors into fluent, policy-compliant natural-language queries with history-aware deduplication. Together, these three stages form a practical instantiation of the adaptive greedy policy for ASCP.

Experiments across diverse deployments show that RAGCRAWLER substantially improves RAG knowledge-base stealing effectiveness. Across four datasets and four RAG generators (including safeguard variants), it achieves up to 84.4% corpus coverage within a 1,000-query budget with BGE retriever. It improves coverage by 44.90% relative to the best baseline and reduces the queries needed to reach 70% coverage by at least 4.03 \times on average. The stolen content also supports service replication: a surrogate RAG built from the recovered corpus reaches up to 0.699 answer similarity to the victim system. RAGCRAWLER is scalable to other RAG techniques like retriever switching, query rewriting, and multi-query retrieval.

Our contribution.

- **Theory.** We formalize RAG knowledge-base stealing as RAG Crawling, an adaptive stochastic coverage problem. We provide a principled, objective, and theoretical grounding for coverage-maximizing black-box attacks.
- **System.** We design RAGCRAWLER, a knowledge graph-guided crawler that instantiates the adaptive greedy coverage principle under real-world constraints.
- **Evaluation.** We conduct extensive evaluations across diverse settings to demonstrate the effectiveness of RAGCRAWLER, as well as against modern RAG defenses.

2 Motivating Example

Consider an attacker targeting a paid support troubleshooting RAG assistant, which is backed by a vendor support portal (Fig. 1(a)). Such portals are often built on private issue tracking tickets and internal resolution notes, and are usually considered IP assets [8]. In our example, we will select three representative issues and assign an icon to each.  (storage),  (replication), and  (authentication) represent three issues. The attacker’s goal is to steal as much of the hidden knowledge base as possible through multi-round queries. By repackaging the stolen knowledge, attackers can mount further downstream attacks such as rehosting the RAG system, bypassing access controls, undercutting subscriptions, or violating licensing and trade secret protections [76].

Existing stealing attacks mainly rely on two local heuristics, **continuation expansion** and **keyword expansion**. In the first strategy (e.g., RAGThief [32]), the new query is built on the context of existing answers. The problem of this strategy is that the query can easily **drift away** from the actual corpus content. For example, in Fig. 1 (a), the last answer about Issue  attributes the failure to a dependency package . A

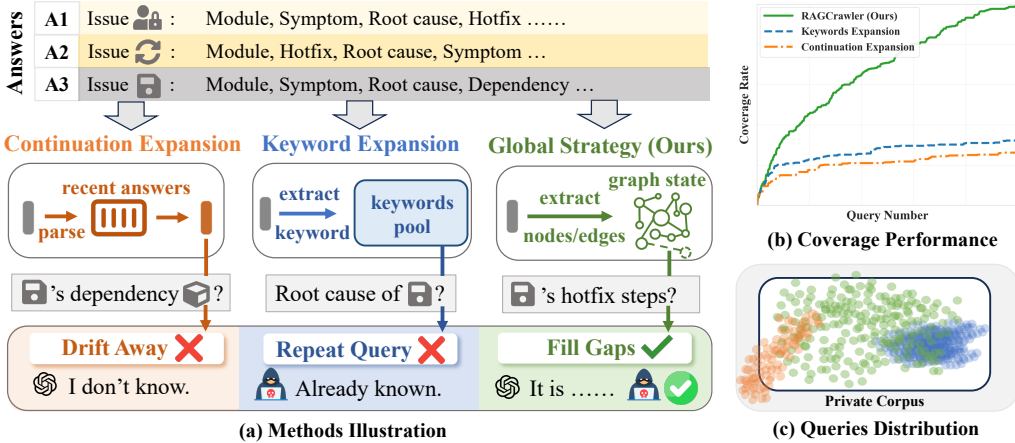


Figure 1: **A motivating example.** (a) A RAG knowledge-base stealing scenario on an IP-bearing troubleshooting corpus. Upper answers represent knowledge obtained from earlier attack rounds. The continuation strategy follows the recent answer, which can drift away from the corpus; the keyword strategy pivots on extracted keywords, often yielding redundant information from the same semantic region; our proposed strategy maintains a global graph, detects unrevealed facts and targets them with new queries. (b) Knowledge coverage w.r.t query number for each strategy on an example corpus. (c) Distribution of retrieved document in the corpus’ semantic space. Each point is a document, with colors indicating queries from different strategies.

continuation-based attacker will ask about \square next, but since it is not in the licensed knowledge base’s scope, this line of questioning yields no useful information. A **keyword-based strategy** (e.g., IKEA [76]) pivots each new query around key terms of previous answers, keeping it mostly within the same semantic neighborhood of the corpus. For example, in Fig. 1 (a), the keyword-based attack **repeatedly asks** about \square ’s root cause and does not explore new contents.

Our approach maintains a **growing knowledge graph** that summarizes discovered entities and relations for globally-planned exploration. Fig. 2 shows the knowledge graph of our attack. Nodes represent entities (e.g., issues, hotfixes, modules), and edges capture relations or co-occurrences (e.g., issue \rightarrow hotfix). As new answers arrive, the graph is expanded with all new entities or relations. By maintaining this global knowledge state, the attacker can detect gaps in what has been revealed so far. As illustrated in Fig. 2, the knowledge graph

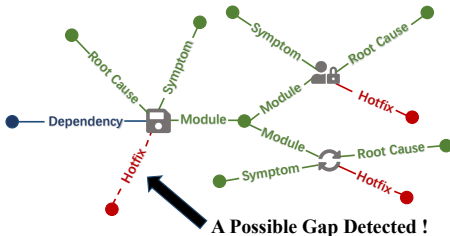


Figure 2: **Illustration of gap detection by the Global Strategy (Ours).** The strategy identifies from the graph that the storage issue (\square) has a missing *Hotfix* facet, and guides the next exploration step to complete this unrevealed knowledge.

dynamically reveals incomplete regions of information. For instance, the graph shows that the issue \square has no revealed *Hotfix*, while the other issues (\square and \square) already have their hotfix information identified. Then the next query will be directed to the uncovered data of \square ’s unobserved hotfix steps, expanding overall coverage.

Our empirical results show that using this global knowledge graph significantly improves the coverage rate. Fig. 1 (b) shows the knowledge coverage rate vs. the number of queries for our attack and two baseline strategies. Guided by the global knowledge graph, our attack (green line) converges much faster than continuation-based (orange curve; focusing on unrelated queries) and keyword-based (blue curve; focusing on repetitive queries) strategies. Fig. 1 (c) provides a qualitative view of how each strategy explores the semantic space of the corpus. Each point denotes a document, and the black box indicates the knowledge-base space. Guided by the global knowledge graph, our attack (green points) spread widely across the space and covers many different clusters of information. The continuation-based queries (orange points) follow a narrow path through the space, gradually drifting away from the space center. Keyword-based queries (blue points) form a few dense clusters around specific topics.

3 Background

3.1 Retrieval-Augmented Generation Systems

A Retrieval-Augmented Generation (RAG) system \mathcal{S} typically comprises a generator \mathcal{G} (an LLM), a retriever \mathcal{R} , and a document collection \mathcal{D} . Given a user query q , the retriever \mathcal{R}

begins by producing an embedding for q and based on some similarity function (typically cosine similarity), fetching the k most relevant documents:

$$\mathcal{D}_k(q) = \arg \text{top-}k_{d \in \mathcal{D}} \text{sim}(q, d). \quad (1)$$

where $\text{sim}(\cdot)$ represents the similarity function, and $\arg \text{top-}k$ selects the top- k documents with the highest similarity scores. The generator \mathcal{G} then produces an answer conditioned on the query and retrieved context [40]:

$$a = \mathcal{G}(\text{wrapper}(q, \mathcal{D}_k(q))), \quad (2)$$

where $\text{wrapper}(\cdot, \cdot)$ denotes the system prompt that interleaves q with the retrieved documents.

In practice, deployed RAG pipelines often incorporate guardrails or enhancements. The most commonly used are *query rewriting* and *multi-query retriever*.

Query rewriting [47, 53, 56, 77] transforms the original query to improve retrievability, resolve ambiguity, repair typos, or strip unsafe instructions. The downstream retrieval and generation processes then operate on the rewritten query.

Multi-query retrieval [39, 45] generates multiple paraphrases of the original query and retrieves independently for each, aggregating the results into a candidate pool. Rather than concatenating all retrieved documents, RAG systems typically re-rank candidates to select the most relevant ones, with *Reciprocal Rank Fusion (RRF)* [19] widely used. While not a dedicated defense, multi-query retrieval’s altered retrieval dynamics may change the attack surface.

3.2 Adaptive Stochastic Coverage Problem

The *Adaptive Stochastic Coverage Problem* (ASCP) models budgeted coverage maximization in sequential decision-making under uncertainty. At each step, an agent selects an action, observes what it reveals, and adapts future actions based on the observations so far. The objective is to maximize expected coverage under a limited budget, such as a limited number of actions. An ASCP instance can be specified by:

- **Item universe (\mathcal{U}):** The item universe \mathcal{U} represents the set of all items that are available for coverage.
- **Action space (Q):** The action space Q consists of all possible actions. Each action q can potentially reveal (cover) a subset of items in \mathcal{U} .
- **Stochastic outcome (realization Φ and $O_\Phi(q)$):** Uncertainty is modeled by a latent realization Φ (a “state of the world”) drawn from a distribution. Conditioned on Φ , executing action q reveals an outcome set $O_\Phi(q) \subseteq \mathcal{U}$.
- **Cost and budget ($c(q), B$):** The cost $c(q)$ represents the resources required to perform action q , and B is the total available budget.
- **Coverage function ($f(S, \Phi)$):** The coverage function $f(S, \Phi)$ quantifies the utility of what has been revealed by a set of actions S under realization Φ . For coverage objectives, f is commonly a function of the union $\bigcup_{q \in S} O_\Phi(q)$.

Theorem 1 (Approximation guarantee of adaptive greedy [26, 37, 38, 58, 78]). *Assume f is adaptively monotone and adaptively submodular. Under a cardinality budget B , the adaptive greedy policy π_{greedy} (maximizing CMG at each step) achieves a $(1 - 1/e)$ -approximation to the optimal expected coverage¹ attained by the optimal adaptive policy π^* under same budget.*

We reduce *RAG knowledge-base stealing* to ASCP by formalizing it as *RAG Crawling* (Sec. 5), enabling CMG-based greedy optimization as a principled strategy for globally planned stealing under a query budget.

3.3 Knowledge Graph

Knowledge graph (KG) is a widely-used knowledge representation technology to organize huge amounts of scattered data into structured knowledge. Formally, a KG is a directed, labeled graph $\mathcal{G} = (\mathcal{E}, \mathcal{L}, \mathcal{R})$, where \mathcal{E} is the set of entities, \mathcal{R} is the set of relation types (edge labels), and $\mathcal{L} \subseteq \mathcal{E} \times \mathcal{R} \times \mathcal{E}$ is the set of labeled, directed edges (facts). Each edge $l \in \mathcal{L}$ is a triple (h, r, t) that connects head $h \in \mathcal{E}$ to tail $t \in \mathcal{E}$ via relation $r \in \mathcal{R}$. For example, (Python, `instanceOf`, Programming Language).

Compared with unstructured text, KGs provide schema-aware, canonicalized facts with explicit connectivity and constraints [31]. We leverage the knowledge graph to construct an attacker-side state that makes coverage estimable, constrains exploration to a compact semantic action space, and records provenance for robust, auditable updates.

4 Threat Model

Scenario. As illustrated in Fig. 3, we consider a production RAG system accessed through a black box interface such as an API or chat. Internally, a retriever selects passages or documents from a corpus \mathcal{D} and a generator composes an answer from the query and the retrieved documents [35, 40]. In deployment the generator may rewrite, summarize, or refuse according to guardrails and access policies [10, 39]. The service does not reveal retrieval scores or document identifiers. The attacker has no insider access and interacts as a normal user. The attacker aims to steal as much of \mathcal{D} as possible by steering retrieval to cover new items across turns.

Prior work has identified two classes of such stealing attacks in RAG systems: *Explicit* attacks append overt adversarial instructions to elicit verbatim disclosure of retrieved text [18, 22, 32, 85]. *Implicit* attacks use benign-looking queries and aggregate factual content that the system legitimately returns across turns, reconstructing corpus via paraphrases and fragments [76]. Our focus is the implicit regime, which better matches real usage and evades refusal rules.

Adversary’s Goal. The attacker aims to steal the knowledge base \mathcal{D} as completely as possible while remaining stealthy.

¹ $(1 - 1/e) \approx 0.63$

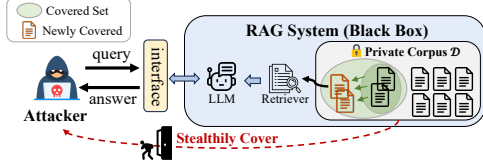


Figure 3: **Threat model.** An external attacker has *black-box* access to a deployed RAG system and can only interact via its public query interface. For each query, the retriever selects a set of documents from the corpus and the LLM generates an answer conditioned on these documents. Across turns, the attacker aims to stealthily expand the union of leaked retrieved items under a query budget.

Leakage may appear as verbatim text, paraphrases, summaries, or factual statements grounded in retrieved documents. At round t , the adversary submits q_t and the system internally consults a hidden retrieved set $\mathcal{D}_k(q_t) \subseteq \mathcal{D}$ to generate the answer. Over B queries, the objective is to maximize the fraction of unique retrieved items:

$$\max_{\{q_1, \dots, q_B\}} \frac{|\bigcup_{t=1}^B \mathcal{D}_k(q_t)|}{|\mathcal{D}|} \quad (3)$$

The budget B models practical constraints such as API cost and the need to limit suspicious activity.

Adversary’s Capabilities. We assume black box access: the attacker submits adaptive natural language queries and observes only final answers. They have no access to retrieval scores, identifiers, indices, or intermediate states, and they cannot modify the retriever or poison the corpus. Following prior work [18, 32, 76], we assume a coarse topic phrase of the target knowledge base is known, as it is often exposed by product descriptions, onboarding pages, or brief interaction. We also evaluate a weaker attacker with no topic prior that issues one benign probe query and compresses the response into a short topic phrase using an attacker-side LLM (the probe counts toward the budget; Appendix D).

5 Reducing RAG Crawling to ASCP

We formalize the attacker’s goal as *RAG Crawling* and reduce it to ASCP (Sec. 3.2). In this way, coverage-maximizing adaptive greedy policies can provide a principled benchmark. We instantiate the ASCP components as follows:

- **Item universe (\mathcal{U}).** We set $\mathcal{U} := \mathcal{D}$, the attacker-hidden corpus, where each item is an atomic document or passage.
- **Action space (\mathcal{Q}).** We set \mathcal{Q} to be the set of all valid natural-language queries the attacker may issue to the victim RAG.
- **Stochastic outcome (realization Φ and $O_\Phi(q)$).** Let Φ denote a latent realization of the victim RAG pipeline that determines retrieval outcomes (including any nondeterminism and attacker-unknown processing such as rewriting or

multi-query retrieval). Conditioned on Φ , issuing query q leads the pipeline to use a hidden set of k retrieved items to generate the final answer; we denote this outcome by

$$O_\Phi(q) := \mathcal{D}_k^\Phi(q) \subseteq \mathcal{D}. \quad (4)$$

- **Cost and budget** ($c(q), B$). We assume unit query cost $c(q) = 1$, so the attacker can issue at most B queries. This matches common deployment settings where the service API charges on a per-query basis: each query consumes one billable request regardless of its exact content.
- **Coverage function** ($f(S, \Phi)$). For a set of queries $S \subseteq \mathcal{Q}$ and realization Φ , the coverage function is

$$f(S, \Phi) := \left| \bigcup_{q \in S} O_\Phi(q) \right|, \quad (5)$$

which matches adversary’s goal (Eq. 3) up to a constant.

We next define conditional expected marginal gain (CMG) as follows. CMG is the oracle quantity optimized by adaptive greedy in ASCP.

Definition 1 (Conditional Expected Marginal Gain in RAG Crawling). *Let ψ_{t-1}^R denote the current retrieval-level partial realization (i.e., the executed query–outcome pairs under the latent realization Φ) after $t-1$ issued queries, and let $S_{t-1} \subseteq \mathcal{Q}$ be the set of queries issued so far. The conditional expected marginal gain (CMG) of a new query $q \in \mathcal{Q}$ given ψ_{t-1}^R is*

$$\Delta(q \mid \psi_{t-1}^R) := \mathbb{E}_{\Phi \mid \psi_{t-1}^R} [f(S_{t-1} \cup \{q\}, \Phi) - f(S_{t-1}, \Phi)]. \quad (6)$$

We then show that RAG Crawling satisfies the assumptions required by ASCP’s greedy approximation theory.

Theorem 2 (Adaptive Monotonicity and Submodularity in RAG Crawling). *The RAG Crawling problem instance satisfies adaptive monotonicity and adaptive submodularity.*

The proof can be found in Appendix A. Building on Theorem 1 and Theorem 2, we have the following:

Theorem 3 (Near-optimality guarantee of the adaptive greedy policy for RAG Crawling). *The adaptive greedy policy for RAG Crawling, which at each step t selects a query*

$$q_t \in \arg \max_{q \in \mathcal{Q}} \Delta(q \mid \psi_{t-1}^R), \quad (7)$$

achieves a $(1 - 1/e)$ -approximation to the optimal expected coverage under the same query budget.

6 RAGCRAWLER

Theorem 3 provides a theoretical guarantee on optimal coverage of RAG Crawling. We now present RAGCRAWLER, which instantiates the adaptive greedy policy for RAG knowledge-base stealing and enables real-world attacks that achieve 66.8% coverage on average with only 1,000 queries.

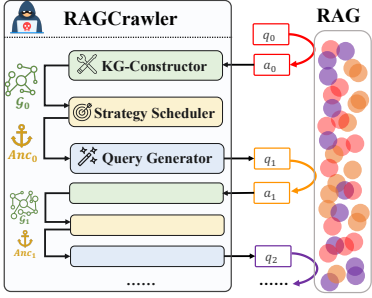


Figure 4: **The workflow of RAGCRAWLER.** At each step, (1) The KG-Constructor processes the latest system response to update the knowledge graph. (2) The Strategy Scheduler analyzes this graph to select a strategic anchor. (3) The Query Generator uses this anchor to formulate the next query.

6.1 Overview

In this section, we explain the workflow of RAGCRAWLER (Fig. 4). RAGCRAWLER implements a closed-loop crawler that alternates between graph state estimation, anchor scheduling, and natural query realization.

At round t , the attacker issues q_t and observes only the answer text a_t , while the retrieved documents remain hidden in the black-box setting. Each answer a_t is processed by **KG-Constructor** to extract a step-wise knowledge subgraph and update the attacker-side state to G_t . Based on G_t , the **Strategy Scheduler** selects a semantic anchor Anc_t to approximate which direction is likely to yield high *marginal coverage gain* in subsequent queries, where we define $Anc_t \triangleq (e_t^*, r_t^*)$ as an entity with an optional relation target. Finally, the **Query Generator** realizes Anc_t into a fluent and policy-compliant query q_{t+1} , sends it to the victim RAG, and the loop repeats. To bootstrap a non-empty graph state, we run a brief topic conditioned seeding phase that generates a few broad queries, and all seeds count toward the budget.

This adaptive loop systematically addresses the three challenges of the ASCP framework. Next, we elaborate on the specific mechanisms employed for each challenge.

6.2 KG-Constructor

This module addresses the first challenge in the ASCP formulation: *the CMG of the attacker’s action is unobservable*. Since the attacker cannot directly observe which documents have been retrieved by the RAG system, the true coverage increment of each query remains hidden.

KG-Constructor makes coverage gains estimable by converting answer text into an attacker-side knowledge graph that compactly summarizes revealed content. Specifically, we maintain an evolving graph state G_t that approximates the latent coverage function $f(S, \Phi)$, making CMG estimable from surface-level answers. The workflow is shown in Fig. 5.

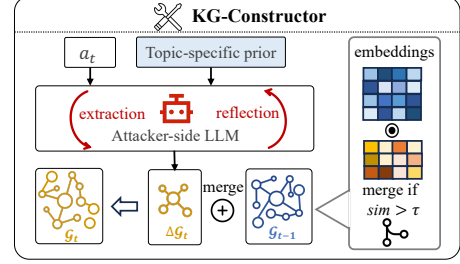


Figure 5: **KG-Constructor.** Guided by a Topic-Specific Prior, the iterative extraction and reflection process generates a knowledge subgraph (ΔG_t), which is then refined through incremental graph update to produce the final graph state G_t .

Why existing approaches do not work. Existing KG construction pipelines do not fit our setting because we require consistent, lightweight incremental updates from partial and evolving answers, without access to the underlying corpus. OpenIE-style extraction [83] produces free-form relations that drift across rounds, causing redundancy and unstable typing, while schema-constrained methods [71] reduce variance but typically assume a fixed ontology and full-data access. LLM-based construction [12, 65] and graph-augmented RAG frameworks (e.g., GraphRAG [24], LightRAG [28]) mainly target one-shot document parsing and retrieval quality, and thus do not provide compact, efficient coverage tracking over many rounds of dynamic responses.

Our methods. Our KG-Constructor supports efficient incremental maintenance by extracting a per-answer subgraph and merging it into the global graph. At round t , the attacker treats the observed answer a_t as the only evidence and extracts a typed triple set $\{(h, r, t)\}$, where h and t are entity mentions (or attribute values) and r is a semantic relation type. We build a knowledge delta ΔG_t using unique h/t mentions as nodes and triples as directed edges, and merge it into G_{t-1} to obtain G_t without rebuilding from scratch. As shown in Fig. 5, the workflow has three modules:

1) Topic-Specific Prior. We derive a lightweight topic-specific schema prior to keep extraction focused and consistent across rounds. Given only a coarse topic signal, we instruct an attacker-side LLM to propose a compact set of entity categories and relation types for the domain (e.g., *disease*, *symptom*, *treatment*, and relations such as *has_symptom*, *treated_by*). During extraction, the LLM prioritizes these schema elements as soft constraints, filtering off-topic content and keeping triples within the topical boundary. This schema stabilizes relation typing across rounds and keeps prompts compact because the LLM conditions on the abstract schema rather than the full graph, reducing overhead while preserving topical precision.

2) Iterative Extraction and Reflection. This component uses the attacker-side LLM to process the new answer. To reduce missing edges caused by conservative extraction, we adopt

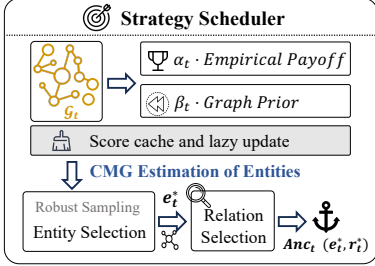


Figure 6: **Strategy Scheduler**. The scheduler selects an action from the graph \mathcal{G}_t via a two-stage process. First, it samples an entity (e_t^*) based on a score that estimates CMG by balancing two key metrics. Second, it selects a relation (r_t^*) by identifying the entity’s largest local information deficit. A score cache with lazy updates ensures the efficiency of this process.

a multi-round extraction–reflection procedure. As shown in Fig. 5, each answer is first processed by an “extraction” pass, and then reprocessed through a “reflection” pass that revisits the same content with awareness of previously omitted facts. This reflection loop enables the LLM to infer implicitly expressed relations and produce additional triples, forming a more comprehensive knowledge subgraph ΔG_I .

3) Incremental Graph Update and Semantic Merging. We finally update the global graph by merging $\Delta\mathcal{G}_t$ into \mathcal{G}_{t-1} with a lightweight attacker-side operation. This integration is implemented as a lightweight merging operation without rebuilding graph from scratch. To ensure that the graph structure reflects genuine semantic expansion rather than redundant surface-level variations, we perform a semantic merging stage. All entity mentions and relation phrases are encoded into a shared embedding space using a pre-trained encoder. Node or edge pairs whose cosine similarity exceeds a threshold τ are automatically identified and merged.

This normalization consolidates synonymous mentions across rounds, keeps G_t compact and stable for CMG estimation and planning space for Strategy Scheduler (Sec. 6.3).

6.3 Strategy Scheduler

This module addresses the second challenge of the ASCP formulation: *attacker action space is intractable*. Operating on the knowledge graph from the KG-Constructor, its task is to select the optimal entity-relation pair (e.g., $(\text{Fix}, \text{HotFix})$) to guide the next query. The challenge is the space of potential strategic actions is combinatorially vast, rendering a brute-force search for the optimal pair computationally infeasible.

Our key insight is *an asymmetry between entities and relations*: entities are the primary drivers of coverage expansion, while relations refine the exploration direction. Exploiting this asymmetry, we reframe the problem into a hierarchical two-stage decision: first select an entity, then pick its unexplored relation to probe. The workflow is shown in Fig. 6.

Entities Selection. We estimate the utility of each entity in \mathcal{G}_t using two complementary metrics: *empirical payoff* and *graph prior*. The *empirical payoff* captures historical information gain and reflects how informative an entity has been in past queries. The *graph prior* exploits the topology of the knowledge graph to identify entities located in structurally under-explored regions. We combine them into a composite score and sample the anchor entity from a Top- K softmax distribution to preserve diversity under noisy estimates.

Empirical payoff. We define the empirical payoff of an entity e via an upper-confidence style score:

$$\text{EmpiricalPayoff}(e) = \bar{g}_e + c \sqrt{\frac{\log N}{n_e + 1}}, \quad (8)$$

where n_e is the number of times e has been selected as the anchor, N is the total number of anchor selections so far, and $c > 0$ controls the strength of the bonus [9, 36].

We define \bar{g}_e as the average normalized graph growth observed when selecting e :

$$\bar{g}_e = \frac{1}{\max(1, n_e)} \sum_{i \in I(e)} \left(\frac{\Delta E_i}{\Delta E_{\max} + \varepsilon} + \frac{\Delta R_i}{\Delta R_{\max} + \varepsilon} \right), \quad (9)$$

where $I(e)$ is the set of rounds in which e served as the anchor, and ΔE_i and ΔR_i are the numbers of newly added entities and relation types in round i after semantic merging. To make gains comparable across rounds, we normalize by window maxima computed over the most recent t_w rounds, denoted by \mathcal{W}_t , i.e., $\Delta E_{\max} = \max_{j \in \mathcal{W}_t} \Delta E_j$ and $\Delta R_{\max} = \max_{j \in \mathcal{W}_t} \Delta R_j$.

Graph prior. While the *empirical payoff* provides a self-contained mechanism for balancing exploitation and statistical exploration, it remains blind to the underlying topology of the knowledge graph. Therefore, we introduce a complementary, structure-aware exploration term: the *graph prior*. This prior injects topological intelligence into the strategy, directing it toward graph regions with high discovery potential. It is composed of two distinct terms:

$$\text{GraphPrior}(e) = \text{DegreeScore}(e) + \text{AdjScore}(e). \quad (10)$$

The first term, `DegreeScore`, promotes exploration in less-dense regions. It penalizes highly connected entities, operating on the intuition that these “hub” nodes are more likely to be information-saturated:

$$\text{DegreeScore}(e) = 1 - \frac{\deg(e)}{\max_{u \in E} \deg(u) + \epsilon}. \quad (11)$$

The second term, AdjScore , directly measures an entity's relational deficit. This deficit quantifies how common a specific relation type is among an entity's peers, given that the entity itself lacks that relation. A high AdjScore thus signals a significant discovery opportunity, prioritizing entities that are most likely to form a new, expected type of connection:

$$\text{AdjScore}(e) = \max_{r \in \mathcal{R}_t} \text{Deficit}(e, r), \quad (12)$$

where the deficit for a specific relation r is defined as:

$$\text{Deficit}(e, r) = \begin{cases} 0, & \text{if } r \in \text{EdgeType}(e), \\ \frac{1}{|\mathcal{E}_{e, \text{type}}|} \sum_{u \in \mathcal{E}_{e, \text{type}}} \#\text{Edge}(u, r), & \text{if } r \notin \text{EdgeType}(e). \end{cases} \quad (13)$$

Here, \mathcal{R} denotes the set of relation types currently in the graph \mathcal{G}_t , $\text{EdgeType}(e)$ is the set of relation types already connected to e , and $\mathcal{E}_{e, \text{type}}$ is the set of all entities sharing the same semantic type as e .

Entity scoring and sampling. We integrate *empirical payoff* and *graph prior* into a final composite score using time-varying weights:

$$\text{Score}(e) = \alpha_t \cdot \text{EmpiricalPayoff}(e) + \beta_t \cdot \text{GraphPrior}(e), \quad (14)$$

where α_t gradually increases with time step t to favor high-confidence anchors in later stages, while β_t remains positive to maintain structural awareness.

To mitigate the risk of prematurely converging on a seemingly optimal path due to noisy gain estimates, we sample the anchor entity e_t^* from a Top- K softmax distribution over the candidate scores, enhancing strategic diversity and robustness.

Relation Selection. Given the sampled anchor e_t^* , we choose a relation by probing its largest local deficit:

$$r^*(e_t^*) = \arg \max_{r \in \mathcal{R} \setminus \text{EdgeType}(e_t^*)} \text{Deficit}(e_t^*, r). \quad (15)$$

To focus on meaningfully large gaps, we compare this maximum to the global distribution of current deficits,

$$\mathcal{DS}_t = \{ \text{Deficit}(e, r) : e \in \mathcal{E}_t, r \in \mathcal{R} \setminus \text{EdgeType}(e) \}, \quad (16)$$

and set $r_t^* = r^*(e_t^*)$ only if it exceeds the 90th percentile of \mathcal{DS}_t ; otherwise, we set $r_t^* = \emptyset$ to indicate that no single relation is a sufficiently promising target.

Ultimately, the scheduler outputs the pair (e_t^*, r_t^*) , which provides structured guidance to Query Generator (Sec. 6.4).

Optimization. We keep scheduling scalable by caching entity scores and lazily recomputing only affected entries after each graph update. When \mathcal{G}_t is updated, we invalidate the cache for entities whose neighborhoods changed, and we reuse cached scores for all other entities. This reduces per-round overhead and decouples scheduling cost from the full graph size.

6.4 Query Generator

This module addresses the third challenge in the ASCP formulation: *Real-world RAG systems impose practical constraints*. We cannot directly send a structured anchor Anc_t to the system, and relying solely on simple templates is not a viable solution, as it can easily be flagged by query provenance mechanisms. Therefore, the core task of this module is to translate the abstract, strategic anchor pair from the Strategy Scheduler into a concrete, executable, and natural-sounding query q_{t+1} .

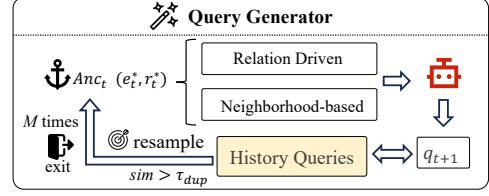


Figure 7: **Query Generator.** Given an anchor pair (e_t^*, r_t^*) , it selects a generation strategy. A candidate query q_{t+1} is produced and checked against historical queries. If redundant, it requests a new anchor from the scheduler and resamples.

This process must address two primary challenges: 1) generating a query that is contextually relevant to the anchor's strategic intent, and 2) ensuring the query remains novel to avoid redundancy under the limited query budget. To achieve this, the generator (Fig. 7) involves the following three steps.

1) Adaptive Query Formulation. The generator's first step is to intelligently select a formulation strategy based on the specificity of the anchor (e_t^*, r_t^*) provided by the scheduler. This dual-mode approach allows the system to flexibly switch between precision and discovery:

- Relation-Driven Probing.** When the Strategy Scheduler identifies a plausible relation deficit r_t^* for an entity e_t^* with high confidence, the generator activates this targeted strategy. It instantiates a relation-aware template conditioned on the (e_t^*, r_t^*) pair and realizes it via an LLM into a fluent, natural language query q_{t+1} designed for precise fact-probing.

- Neighborhood-based Generation.** In the absence of a sufficiently salient relation, the generator shifts to an exploratory mode. It analyzes the local neighborhood of e_t^* within the current knowledge graph \mathcal{G}_t . By leveraging the KG's schema and the generative capabilities of LLM, it hypothesizes plausible missing relations and formulates one or more exploratory query variants.

2) History-aware De-duplication To maximize the information yield of each query, we introduce a robust quality control gate powered by a history-aware resampling loop. Before being dispatched, each candidate query q is compared against the historical query log Q_{hist} . If its similarity $\text{sim}(q, Q_{\text{hist}}) \geq \tau_{\text{dup}}$, the generator triggers a resample operation, drawing a new anchor from the Strategy Scheduler's Top- K distribution and re-attempting the formulation, up to M trials. This mechanism is critical for avoiding diminishing returns. If all M trials yield near-duplicate queries, we treat the current exploration as saturated. As a practical fallback, an attacker can either restart a seeding step to diversify the query pool [32, 76], or terminate early to avoid wasting the remaining query budget.

3) Penalties and Feedback Loop. We close the loop by feeding generation outcomes back into scheduling. When a query is refused, yields an empty answer, or is rejected as a duplicate, we apply a strategy-specific penalty to the corresponding payoff update so that such anchors become less likely to be

selected in future rounds. This feedback lets the planner adapt away from unproductive regions and toward anchors that reliably produce new graph growth.

7 Evaluation

We conduct comprehensive experiments to answer the following research questions:

RQ1: How effective is RAGCRAWLER compared with existing attack methods?

RQ2: How does the retriever in the victim RAG affect stealing performance?

RQ3: How does the attacker-side LLM agent influence stealing performance?

RQ4: How robust is the attack against RAG variants employing query rewriting or multi-query retrieval?

RQ5: How do hyperparameters and individual techniques affect the effectiveness of RAGCRAWLER?

7.1 Evaluation Setup

Dataset. We evaluate on four corpora spanning diverse domains with varying styles and scales. TREC-COVID and SciDocs are from BEIR [73] with 171.3K and 25.6K documents, and NFCorpus [13] with 5.4K documents. We additionally include Healthcare-Magic-100k [4] (Healthcare) with about 100K patient-provider Q&A samples. Together they cover biomedical literature, scientific papers, consumer health, and clinical dialogues. For efficiency and fair comparison, we randomly sample 1,000 de-duplicated documents from each corpus to form the victim RAG collection [22, 32]. We verify that each subset preserves the full-corpus semantic distribution using Energy Distance [72] and C2ST [51] (Appendix B), and report results with larger victim collections in Appendix E.4.

Generator and Retriever. We employ two retrievers in our evaluations: BGE [87] and GTE [44]. For generators, we evaluate four large language models: Llama 3.1 Instruct-8B (denoted as Llama-3-8B) [23], Command-R-7B [3], Microsoft-Phi-4 [1], and GPT-4o-mini [61]. These generators cover both open-source and proprietary systems and span different model families and sizes. Including GPT-4o-mini, which incorporates safety guardrails [62], allows us to evaluate whether stealing remains feasible under built-in guardrails.

Attacker-side LLM. We adopt two attacker-side LLMs to simulate query generation. In the main experiments, we use Doubao-1.5-lite-32K [14] due to its high speed, cost efficiency, and independence from the RAG’s generator family (aligns with the black-box assumption). We also evaluate a smaller open-source alternative, Qwen-2.5-7B-Instruct [67], to examine transferability between model families and sizes.

RAG Setting. We consider three victim configurations: vanilla RAG, query rewriting, and multi-query retrieval with RRF re-ranking (default: 3 query variants per user request).

We set retrieval depth to $k = 10$ by default and analyze the impact of k in Sec. 7.6. The retrieved documents are provided to the generator as contextual input through a structured system prompt. Further details are provided in Appendix F.

Baselines. We compare RAGCRAWLER against two state-of-the-art black-box RAG knowledge-base stealing attacks: RAGThief [32] and IKEA [76]. RAGThief represents continuation-based attack, and IKEA represents keyword-based attack. To ensure fair comparison, all attacks use the same attacker-side LLM, and we adopt default hyperparameters from the original papers. Unless otherwise specified, each attack is allowed to issue at most 1,000 queries to the victim RAG, ensuring consistent query budgets across methods.

Metrics. We evaluate stealing along four complementary axes: exposure breadth, semantic faithfulness of the stolen content, query cost to reach target coverage, and whether the extracted corpus can support service replication.

Coverage Rate (CR) measures the fraction of the corpus exposed through retrieval, matching Eq. 3; refusals are treated as empty outcomes as in [32, 76].

Semantic Fidelity (SF) measures average semantic overlap between each document $d \in \mathcal{D}$ and the stolen content \mathcal{A} , where \mathcal{A} is the set of answer snippets produced across all issued queries, using a fixed encoder $E_{\text{eval}}(\cdot)$:

$$s(d) = \max_{e \in \mathcal{A}} \cos(E_{\text{eval}}(d), E_{\text{eval}}(e)). \quad (17)$$

Target-Coverage Query Complexity Q_γ is the minimum number of issued queries needed to reach coverage γ (the first t such that $\text{CR}(t) \geq \gamma$). When the target is not reached under a cap Q_{\max} , we treat Q_γ as right-censored and report $Q_\gamma > Q_{\max}$.

Reconstruction Fidelity assesses whether the stolen corpus supports service replication. We build a surrogate RAG from the stolen content and evaluate it on official query annotations of TREC-COVID, SciDocs, and NFCorpus, restricted to the sampled documents (1,860, 2,181, and 1,991 queries). Healthcare is excluded due to the lack of official query annotations. We report success rate (fraction of non-refusal responses), answer similarity (semantic similarity between surrogate and victim answers), and ROUGE-L.

7.2 Effectiveness (RQ1)

We evaluate the effectiveness of RAGCRAWLER through corpus coverage, semantic fidelity, target-coverage query complexity, and reconstruction fidelity. Across all evaluations, RAGCRAWLER demonstrates the strongest performance.

Coverage Rate. Under a fixed 1,000-query budget with the BGE retriever, RAGCRAWLER attains the highest final coverage in every configuration in Table 1. Averaged over all 16 configurations, RAGCRAWLER exposes 66.8% of the corpus, compared with 46.1% for IKEA and 9.6% for RAGThief. The margin is largest on harder corpora (TREC-COVID), where RAGCRAWLER reaches 49.4% average coverage across generators, while IKEA remains at 18.2%. The coverage curves

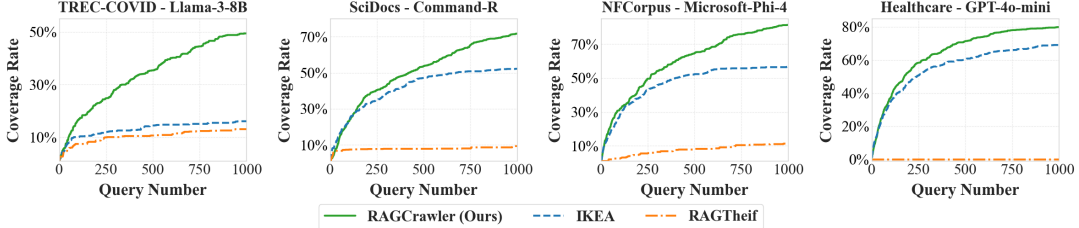


Figure 8: Coverage Rate vs. Query Number (1,000 Budget) across datasets and generators (BGE Retriever). RAGCRAWLER steadily increases coverage and consistently surpasses both RAGThief and IKEA. Full results are in Fig. 11.

Table 1: Coverage rate (CR) and semantic fidelity (SF) of attacks under a 1,000-query budget (victim retriever: BGE) across four datasets and four generators. Abbreviations: Gen (Generator), TREC-C (TREC-COVID), Cmd-R (Command-R), MS-Phi (Microsoft-Phi-4), 4o-mini (GPT-4o-mini). “N/A” indicates undefined semantic fidelity due to zero coverage. RAGCRAWLER performs best in every setting.

Dataset	Gen	CR			SF		
		RAGThief	IKEA	RAGCrawler	RAGThief	IKEA	RAGCrawler
TREC-C	Llama	0.131	0.161	0.494	0.447	0.495	0.591
	Cmd-R	0.154	0.173	0.544	0.444	0.525	0.614
	MS-Phi	0.121	0.197	0.474	0.468	0.547	0.619
	4o-mini	0.000	0.197	0.465	N/A	0.543	0.572
SciDocs	Llama	0.053	0.513	0.661	0.264	0.495	0.523
	Cmd-R	0.093	0.522	0.717	0.295	0.514	0.561
	MS-Phi	0.065	0.545	0.711	0.324	0.534	0.563
	4o-mini	0.000	0.421	0.516	N/A	0.475	0.492
NFCorpus	Llama	0.061	0.503	0.797	0.451	0.644	0.698
	Cmd-R	0.169	0.517	0.844	0.467	0.656	0.705
	MS-Phi	0.113	0.566	0.813	0.487	0.663	0.717
	4o-mini	0.000	0.493	0.631	N/A	0.631	0.653
Healthcare	Llama	0.361	0.687	0.807	0.536	0.588	0.618
	Cmd-R	0.170	0.592	0.766	0.383	0.578	0.582
	MS-Phi	0.052	0.588	0.654	0.434	0.558	0.599
	4o-mini	0.000	0.693	0.799	N/A	0.490	0.577
Average		0.096	0.461	0.668	0.417	0.559	0.605

in Fig. 8 further indicate that RAGCRAWLER continues to accrue new documents throughout the process, whereas baselines typically flatten earlier, consistent with diminishing returns from locally reactive querying.

RAGCRAWLER also remains effective under generators with built-in guardrails. When the victim generator is GPT-4o-mini, RAGThief yields zero coverage across all four corpora, while RAGCRAWLER still reaches 46.5%–79.9% coverage, suggesting that benign, policy-compliant probing can sustain stealing even when overt jailbreak patterns are blocked.

Semantic Fidelity. Higher coverage does not come at the expense of semantic quality. Across all dataset–generator pairs, RAGCRAWLER achieves the highest average SF (0.605), exceeding IKEA (0.559) and RAGThief (0.417) in Table 1.

Target-Coverage Query Complexity. We next evaluate query efficiency for reaching high coverage targets. Table 2 reports $Q_{0.7}$ under a cap $Q_{\max} = 5,000$. RAGCRAWLER is the only method that reaches 70% coverage on all datasets within

Table 2: Target-coverage query complexity to reach 70% coverage ($Q_{0.7}$) under a cap $Q_{\max} = 5,000$ (victim: Llama-3-8B generator, BGE retriever). Entries marked “ $> Q_{\max}$ ” are right-censored, with the achieved coverage shown in parentheses. The full sweep of Q_{γ} is reported in Tab. 10. RAGCRAWLER reaches high coverage with far fewer queries.

Dataset	RAGThief	IKEA	RAGCrawler
TREC-COVID	$> 5,000$ (29.8%)	$> 5,000$ (19.6%)	4,040
SciDocs	$> 5,000$ (7.2%)	$> 5,000$ (56.0%)	1,163
NFCorpus	$> 5,000$ (16.5%)	$> 5,000$ (64.0%)	595
Healthcare	$> 5,000$ (53.0%)	1,231	568

the cap, requiring 4,040 queries on TREC-COVID and at most 1,163 queries on the other corpora (595 on NFCorpus and 568 on Healthcare). IKEA reaches 70% only on Healthcare (1,231 queries) and stays below 70% elsewhere even at Q_{\max} , while RAGThief never reaches 70%. Relative to the strongest baseline per dataset, RAGCRAWLER reduces $Q_{0.7}$ by 2.17× on Healthcare and by at least 1.24×, 4.30×, and 8.40× on TREC-COVID, SciDocs, and NFCorpus (lower bounds due to censoring). This translates to average $\geq 4.03 \times$ reduction in monetary cost under linear per-request pricing (e.g., \$20 per 1,000 search requests on Vertex AI Search [27]).

The full sweep in Tab. 10 highlights the gap. While IKEA can be competitive at low targets on easier corpora (e.g., Healthcare $Q_{0.5} = 212$ vs. 209), it saturates as γ increases and fails to reach 90% on any dataset within Q_{\max} . In contrast, RAGCRAWLER reaches 90% on SciDocs, NFCorpus, and Healthcare with 3,330, 1,753, and 2,434 queries, respectively, and attains 72.5% final coverage on TREC-COVID, more than doubling the best baseline’s (29.8% for RAGThief).

Reconstruction Fidelity. To test whether the stolen corpus enables service replication, we build surrogate RAG systems from each method’s stolen outputs and evaluate them on held-out query sets. Table 3 shows that surrogates built from RAGCRAWLER achieve substantially higher success rates (38.1%–52.6%) and consistently higher answer similarity and ROUGE-L, with peaks of 0.6992 similarity and 0.2408 ROUGE-L. Notably, on SciDocs the IKEA-based surrogate has a very low success rate (0.0179) despite IKEA reaching 51.3% coverage under the 1,000-query budget in Table 1, indi-

Table 3: Reconstruction fidelity of surrogate RAG systems built from *stolen* knowledge-base content (victim: Llama-3-8B generator, BGE retriever). We report success rate (non-refusal), answer embedding similarity, and ROUGE-L against victim outputs. Best results are in **bold**. Surrogates built from RAGCRAWLER’s stolen corpus match the victim best.

Dataset	Method	Success Rate	Answer Sim.	ROUGE-L
TREC-COVID	RAGThief	0.1129	0.4920	0.1547
	IKEA	0.2247	0.4779	0.1730
	RAGCrawler	0.3839	0.6098	0.2408
SciDocs	RAGThief	0.0486	0.4275	0.1131
	IKEA	0.0179	0.4829	0.1277
	RAGCrawler	0.3810	0.5900	0.2285
NFCorpus	RAGThief	0.0447	0.5156	0.1063
	IKEA	0.4215	0.6064	0.2013
	RAGCrawler	0.5259	0.6992	0.2334

cating that partial theft concentrated in a limited region does not necessarily translate into functional replication. Overall, the reconstruction results align with the coverage and fidelity trends: broader exploration coupled with higher semantic alignment yields stolen corpora that are materially more useful for building a substitute service.

Takeaway. Across datasets and generators, RAGCRAWLER delivers the strongest stealing breadth, semantic fidelity, and query efficiency, and the resulting stolen content transfers into markedly higher-fidelity surrogate reconstruction.

7.3 Retriever Sensitivity (RQ2)

To evaluate the robustness of RAGCRAWLER against different retrieval architectures, we evaluated the attack methods on victim RAG systems with GTE [44] as retriever.

Swapping the retriever shifts the attack surface for all methods, but RAGCRAWLER remains the most effective extractor in terms of coverage. With GTE, RAGCRAWLER achieves 76.6% average coverage across datasets, compared with 53.9% for IKEA and 28.2% for RAGThief (Table 4). The effect of the retriever is not uniform across corpora: relative to BGE, RAGCRAWLER gains 27.1 points on TREC-COVID (49.4% to 76.5%) and 17.2 points on SciDocs (66.1% to 83.3%), but drops by 5.9 and 7.9 points on NFCorpus and Healthcare, respectively. This variation suggests that retriever choice can materially change which parts of a corpus are easy to surface, yet RAGCRAWLER consistently maintains high coverage (at least 72.8%) across all four corpora under GTE.

Semantic fidelity remains broadly stable. Averaged over datasets, RAGCRAWLER attains SF 0.597, exceeding IKEA (0.571) and RAGThief (0.484). The only exception is Healthcare, where IKEA achieves marginally higher SF (0.576 vs. 0.567), indicating that retriever changes can also alter per-document alignment quality in specific domains.

Takeaway. RAGCRAWLER generalizes across retrievers: changing the victim retriever can affect absolute difficulty

Table 4: Coverage rate (CR) and semantic fidelity (SF) of attacks when the victim uses GTE as retriever (generator: Llama-3-8B; 1,000-query budget). Best results are in **bold**. RAGCRAWLER remains dominant.

Dataset	CR			SF		
	RAGThief	IKEA	RAGCrawler	RAGThief	IKEA	RAGCrawler
TREC-COVID	0.191	0.391	0.765	0.453	0.565	0.610
SciDocs	0.162	0.472	0.833	0.345	0.495	0.539
NFCorpus	0.386	0.622	0.738	0.589	0.648	0.671
Healthcare	0.388	0.671	0.728	0.548	0.576	0.567
Average	0.282	0.539	0.766	0.484	0.571	0.597

and the coverage–fidelity balance, but RAGCRAWLER remains the strongest overall threat, especially in coverage.

7.4 Agent Sensitivity (RQ3)

To investigate the influence of the attacker’s LLM agent on attack performance, we evaluated the effectiveness with a smaller open-source model, Qwen-2.5-7B-Instruct.

RAGCRAWLER remains effective with a smaller attacker model. With Qwen-2.5-7B-Instruct (victim: Llama-3-8B, BGE), RAGCRAWLER achieves 71.3% average coverage with 0.585 semantic fidelity (Table 5). Compared to the Doubao agent under the same victim setting, the per-dataset coverage changes are small (within a few percentage points), suggesting that the global scheduler and graph state dominate the attack trajectory, while the LLM agent primarily executes localized, well-specified generation tasks.

In comparison, the baseline methods remain significantly less effective. With the Qwen-2.5-7B-Instruct agent, IKEA achieves an average coverage of 48.0%, while RAGThief reaches 27.5%. Although RAGThief sees a slight performance improvement (likely because the constrained divergent ability of smaller model make it less prone to the off-topic drift), it still lags far behind RAGCRAWLER.

Takeaway. Attack effectiveness for RAGCRAWLER is largely agent-agnostic, reinforcing that its advantage comes from planning and redundancy control rather than relying on a high-capability attacker LLM.

Table 5: Coverage rate (CR) and semantic fidelity (SF) of attacks when using Qwen-2.5-7B-Instruct as the attacker-side agent (victim: Llama-3-8B generator, BGE retriever; 1,000-query budget). Best results are in **bold**. RAGCRAWLER remains dominant.

Dataset	CR			SF		
	RAGThief	IKEA	RAGCrawler	RAGThief	IKEA	RAGCrawler
TREC-COVID	0.271	0.183	0.542	0.469	0.499	0.570
SciDocs	0.099	0.489	0.675	0.298	0.487	0.507
NFCorpus	0.314	0.559	0.834	0.559	0.646	0.678
Healthcare	0.414	0.687	0.799	0.549	0.576	0.584
Average	0.275	0.480	0.713	0.469	0.552	0.585

Table 6: Coverage rate (CR) and semantic fidelity (SF) under practical RAG variants (victim: Llama-3-8B generator, BGE retriever, 1,000-query budget). Best results are in **bold**. RAGCRAWLER remains the strongest attack.

Dataset	Query Rewriting					
	CR			SF		
	RAGThief	IKEA	RAGCrawler	RAGThief	IKEA	RAGCrawler
TREC-COVID	0.381	0.241	0.601	0.519	0.537	0.591
SciDocs	0.561	0.542	0.743	0.442	0.479	0.507
NFCorpus	0.664	0.489	0.854	0.633	0.618	0.687
Healthcare	0.709	0.595	0.767	0.556	0.564	0.577
Average	0.579	0.467	0.741	0.538	0.550	0.591
Dataset	Multi-query Retrieval					
	CR			SF		
	RAGThief	IKEA	RAGCrawler	RAGThief	IKEA	RAGCrawler
TREC-COVID	0.326	0.189	0.474	0.525	0.523	0.581
SciDocs	0.352	0.508	0.697	0.364	0.494	0.514
NFCorpus	0.392	0.540	0.849	0.588	0.631	0.692
Healthcare	0.562	0.605	0.761	0.569	0.580	0.587
Average	0.408	0.461	0.695	0.512	0.557	0.594

7.5 Defense Robustness (RQ4)

To further explore potential defenses, we extend our evaluation beyond the test against GPT-4o-mini’s built-in guardrails (Sec. 7.2) to two practical mechanisms widely adopted by RAG: query rewriting and multi-query retrieval.

Query Rewriting. In this configuration, the victim RAG system employs an LLM to rewrite incoming queries, aiming to clarify user intent and neutralize potential adversarial patterns before retrieval and generation. RAGCRAWLER exhibits exceptional resilience against this defense, maintaining superior performance metrics. As detailed in Table 6, RAGCRAWLER achieves an average coverage rate of 74.1% and semantic fidelity of 0.591. Although intended as a safeguard, the query rewriting process is paradoxically exploited by our method to enhance theft. By explicitly refining the query’s semantic intent, the rewriter enables the retriever to surface a more relevant and diverse set of documents than the original input would yield. RAGCRAWLER’s adaptive planner capitalizes on this context to accelerate corpus exploration; for instance, on the NFCorpus dataset, coverage increases from 79.7% to 85.4% when this defense is active.

In contrast, baseline methods fail to effectively exploit this dynamic. While RAGThief sees its average coverage improve to 57.9% and IKEA reaches 46.7%, both remain significantly behind RAGCRAWLER. RAGThief benefits incidentally, as the rewriting step strips away its obvious adversarial suffixes; however, lacking a strategic framework to systematically capitalize on the enhanced retrieval results, it cannot match RAGCRAWLER’s efficiency, underscoring the fundamental limitations of heuristic-based approaches.

Multi-query Retrieval. We next evaluate against multi-query retrieval, which expands each query into several variants whose retrieved results are re-ranked and fused, a process that

Table 7: Coverage rate (CR) with a provided topic prior vs. a no-prior attacker (victim: Llama-3-8B generator, BGE retriever). Best results are in **bold**. RAGCRAWLER remains best and shows small sensitivity to topic-prior removal.

Method	TREC-COVID		SciDocs		NFCorpus		Healthcare	
	Prior	No-prior	Prior	No-prior	Prior	No-prior	Prior	No-prior
RAGThief	0.131	0.128	0.053	0.040	0.061	0.123	0.361	0.290
IKEA	0.161	0.391	0.513	0.108	0.503	0.536	0.687	0.705
RAGCrawler	0.494	0.426	0.661	0.613	0.797	0.825	0.807	0.755

can influence attack surface. Once again, RAGCRAWLER excels, achieving the highest average coverage of 69.5% and a semantic fidelity of 0.593 (Table 6). This mechanism provides the attacker with a more diverse set of retrieved documents from different semantic clusters. The global graph in RAGCRAWLER is uniquely positioned to exploit this; it integrates this diverse information to build a more comprehensive map of the corpus, thereby generating more effective and far-reaching follow-up queries.

The baseline methods, however, are not equipped to fully leverage this enriched context. RAGThief and IKEA attain coverage rates of 40.8% and 46.1%, respectively. Their localized strategies are unable to fully synthesize the information from the multiple retrieval results.

Takeaway. RAGCRAWLER remains highly effective against practical RAG defenses. The results demonstrate that defenses designed to sanitize inputs or strengthen retrieval can be subverted by a strategic attacker and may even amplify the stealing threat, calling for more advanced safeguards.

7.6 Ablation Study (RQ5)

We analyze how attacker assumptions, efficiency techniques, and victim-side hyperparameters influence RAGCRAWLER’s effectiveness. More ablations on modules and hyperparameter choices are provided in Appendix E.2.

Robustness to topic prior. Our main threat model assumes a coarse topic phrase [18, 32, 76], which is typically exposed by production RAG services. We further evaluate a weaker attacker that starts with no topic prior and infers a coarse 3–8 word topic phrase using a single benign probe query (counted toward the budget). Table 7 shows that RAGCRAWLER remains the best-performing attack in this setting, with only modest CR changes relative to the topic-prior setting. Appendix D details the one-shot probing procedure and analyzes the quality and variability of the inferred topic phrases.

Score Cache. We quantify the computational benefit of caching similarity-score updates inside the strategy scheduler. Figure 9 shows that caching reduces the number of score updates from over 1.67 million to about 0.63 million across datasets, corresponding to a 62% workload reduction (2.67× fewer updates). Because later rounds increasingly revisit overlapping neighborhoods in the evolving graph, the cache bene-

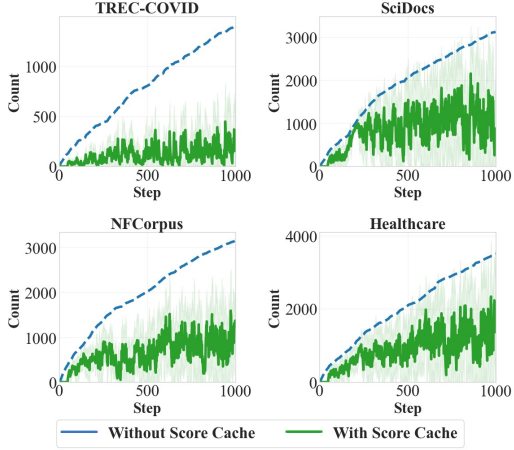


Figure 9: Score Computations with vs. without Caching. Caching reduces the number of similarity score updates by $\sim 2.67 \times$ on average, greatly improving efficiency.

fit grows with interaction length, improving practicality for larger budgets or larger corpora.

Victim Retrieval Depth. We vary the victim retrieval depth k to study how much per-query context expansion affects attack performance. On TREC-COVID, increasing k substantially accelerates early coverage growth: within 1,000 queries, coverage rises from roughly 28% at $k = 5$ to above 60% at $k = 20$ (Fig. 10). However, the curve exhibits diminishing returns as k increases, consistent with additional retrieved documents being increasingly redundant with already exposed content. This result highlights a security implication of aggressive retrieval: larger k increases the amount of unique corpus material that can be exposed per user query.

8 Discussion and Related Work

Cost Analysis. We separate (i) attacker-side orchestration cost (tokens for running RAGCRAWLER) from (ii) victim-side service cost (per-query fees). Tab. 9 shows RAGCRAWLER incurs only \$0.33–\$0.53 per dataset under Doubao-1.5-lite-32K

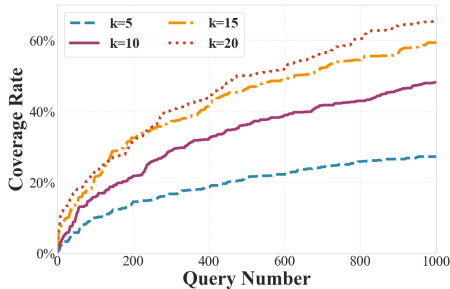


Figure 10: Coverage Rate vs. Query Number for different victim depth k on TREC-COVID, Llama-3-8B, BGE.

pricing, and becomes **near-zero** with open-source models (Sec. 7.4) aside from GPU hosting. Victim-side fees scale linearly with issued queries (e.g., $Q_{0.7}$ in Tab. 2). The low attacker overhead creates strong economic asymmetry against RAG development cost [2], enabling low-cost service piracy.

Scalability. Although production RAG corpora may contain millions of documents, RAGCRAWLER scales because each turn extracts a compact typed delta from the single observed answer to update the attacker-side KG, keeping per-turn LLM cost independent of $|\mathcal{D}|$. The main bottleneck is accumulated-state maintenance (semantic merging and score updates), which we mitigate with caching and lazy recomputation (62% fewer score updates; Fig. 9). For larger budgets, ANN-backed deduplication [54, 82] and out-of-core graph and score storage [5, 81, 86] offer orthogonal engineering extensions.

Defenses. Our attack highlights the inherent limitations of defenses that rely on analyzing queries in isolation (e.g., guardrails or query rewriting). Moreover, when we evaluate an LLM-based intent detector, it flags only **1.07%** of the attack queries as suspicious. The core challenge is that the malicious pattern is an emergent property of the entire interaction sequence, not an attribute of any single query. This exposes a critical blind spot in static security models and argues for a pivot towards dynamic, behavior-aware defenses. Based on this analysis, we believe query provenance analysis [29, 41, 42, 55] holds significant promise. Verifying its practical effectiveness would be a valuable next step for the research community.

Security Risks in RAG. This paper concentrates on knowledge-base stealing attacks against RAG systems [18, 22, 32, 66, 76]. RAG systems are also susceptible to other security risks [59, 74]. Membership Inference Attacks (MIA) enable an adversary to determine if a specific document is present in the corpus, thereby exposing the existence of sensitive records [7, 25, 48, 57]. Furthermore, in Corpus Poisoning attacks, an adversary injects malicious data into the RAG knowledge base [11, 16, 17, 46, 49, 69, 88, 89]. Retrieval of this corrupted data can manipulate the system’s output, allowing the attacker to propagate misinformation or harmful content.

9 Conclusion

We investigated knowledge-base stealing in RAG systems, a growing threat to the intellectual property of the retrieval corpus. We formalized the attacker’s goal as *RAG Crawling*, an instance of ASCP that targets global corpus coverage under a fixed query budget, and we developed RAGCRAWLER, a knowledge graph-guided framework that operationalizes this objective in practical black-box settings. Extensive experiments show that RAGCRAWLER achieves substantially higher coverage than prior attacks (up to 84.4% within a budget of 1,000 queries) and remains effective under query rewriting and multi-query retrieval, highlighting urgent gaps in protecting the knowledge assets of RAG deployments.

References

- [1] Marah Abdin, Jyoti Aneja, Harkirat Behl, Sébastien Bubeck, Ronen Eldan, Suriya Gunasekar, Michael Harrison, Russell J Hewett, Mojan Javaheripi, Piero Kauffmann, et al. Phi-4 technical report. *arXiv preprint arXiv:2412.08905*, 2024.
- [2] ADaSci Research. How to evaluate the rag pipeline cost. <https://adasci.org/how-to-evaluate-the-rag-pipeline-cost>, 2024. Accessed: 2025-11-11.
- [3] Cohere For AI. C4ai-command-r7b-12-2024. <https://huggingface.co/CohereForAI/c4ai-command-r7b-12-2024>, 2024. Open-source large-language model.
- [4] Lavita AI. Chatdoctor-healthcaremagic-100k. <https://huggingface.co/datasets/lavita/ChatDoctor-HealthCareMagic-100k>, 2024. Dataset on Hugging Face.
- [5] Zhiyuan Ai, Mingxing Zhang, Yongwei Wu, Xuehai Qian, Kang Chen, and Weimin Zheng. Squeezing out all the value of loaded data: An out-of-core graph processing system with reduced disk {I/O}. In *2017 USENIX annual technical conference (USENIX ATC 17)*, pages 125–137, 2017.
- [6] Yasmina Al Ghadban, Huiqi Lu, Uday Adavi, Ankita Sharma, Sridevi Gara, Neelanjana Das, Bhaskar Kumar, Renu John, Praveen Devarsetty, and Jane E Hirst. Transforming healthcare education: Harnessing large language models for frontline health worker capacity building using retrieval-augmented generation. *medRxiv*, pages 2023–12, 2023.
- [7] Maya Anderson, Guy Amit, and Abigail Goldstein. Is my data in your retrieval database? membership inference attacks against retrieval augmented generation. In *International Conference on Information Systems Security and Privacy*, volume 2, pages 474–485. Science and Technology Publications, Lda, 2025.
- [8] Atlassian. Jira | issue & project tracking software | atlassian. <https://www.atlassian.com/software/jira>. Accessed: 2026-02-01.
- [9] Peter Auer, Nicolo Cesa-Bianchi, and Paul Fischer. Finite-time analysis of the multiarmed bandit problem. *Machine learning*, 47(2):235–256, 2002.
- [10] Alina Beck. Raising the bar for rag excellence: query rewriting and new semantic ranker. <https://techcommunity.microsoft.com/blog/azure-ai-servicesblog/raising-the-bar-for-rag-excellence-query-rewriting-and-new-semanticranker/4302729/>, 2025. Accessed: 2025-11-04.
- [11] Matan Ben-Tov and Mahmood Sharif. Gasliteing the retrieval: Exploring vulnerabilities in dense embedding-based search. *arXiv preprint arXiv:2412.20953*, 2024.
- [12] Haonan Bian. Llm-empowered knowledge graph construction: A survey. *arXiv preprint arXiv:2510.20345*, 2025.
- [13] Vera Boteva, Demian Gholipour, Artem Sokolov, and Stefan Riezler. A full-text learning to rank dataset for medical information retrieval. In *European Conference on Information Retrieval*, pages 716–722. Springer, 2016.
- [14] ByteDance. Doubao-1.5-lite-32k. <https://www.volcengine.com/docs/82379/1554679>, 2024. Lightweight version of the Doubao-1.5 series by ByteDance.
- [15] Nicholas Carlini, Daniel Paleka, Krishnamurthy Dj Dvijotham, Thomas Steinke, Jonathan Hayase, A Feder Cooper, Katherine Lee, Matthew Jagielski, Milad Nasr, Arthur Conmy, et al. Stealing part of a production language model. *arXiv preprint arXiv:2403.06634*, 2024.
- [16] Harsh Chaudhari, Giorgio Severi, John Abascal, Matthew Jagielski, Christopher A Choquette-Choo, Milad Nasr, Cristina Nita-Rotaru, and Alina Oprea. Phantom: General trigger attacks on retrieval augmented language generation. *arXiv preprint arXiv:2405.20485*, 2024.
- [17] Sukmin Cho, Soyeong Jeong, Jeongyeon Seo, Taeho Hwang, and Jong C Park. Typos that broke the rag's back: Genetic attack on rag pipeline by simulating documents in the wild via low-level perturbations. In *Proceedings of the 2024 Conference on Empirical Methods in Natural Language Processing (EMNLP 2024)*. Association for Computational Linguistics, 2024.
- [18] Stav Cohen, Ron Bitton, and Ben Nassi. Unleashing worms and extracting data: Escalating the outcome of attacks against rag-based inference in scale and severity using jailbreaking. *arXiv preprint arXiv:2409.08045*, 2024.
- [19] Gordon V Cormack, Charles LA Clarke, and Stefan Buettcher. Reciprocal rank fusion outperforms condorcet and individual rank learning methods. In *Proceedings of the 32nd international ACM SIGIR conference on Research and development in information retrieval*, pages 758–759, 2009.
- [20] Shashank Reddy Danda, Xiaoyong Yuan, and Bo Chen. Towards stealing deep neural networks on mobile devices. In *International Conference on Security and Privacy in Communication Systems*, pages 495–508. Springer, 2021.

[21] Madhureeta Das, Gaurav Bagwe, Miao Pan, Kaichen Yang, Xiaoyong Yuan, and Lan Zhang. Siamese: Stealing fine-tuned visual foundation models via diversified prompting. In *Proceedings of the Tenth ACM/IEEE Symposium on Edge Computing*, pages 1–7, 2025.

[22] Christian Di Maio, Cristian Cosci, Marco Maggini, Valentina Poggioni, and Stefano Melacci. Pirates of the rag: Adaptively attacking llms to leak knowledge bases. *arXiv preprint arXiv:2412.18295*, 2024.

[23] Abhimanyu Dubey, Abhinav Jauhri, Abhinav Pandey, Abhishek Kadian, Ahmad Al-Dahle, Aiesha Letman, Akhil Mathur, Alan Schelten, Amy Yang, Angela Fan, et al. The llama 3 herd of models. *arXiv e-prints*, pages arXiv–2407, 2024.

[24] Darren Edge, Ha Trinh, Newman Cheng, Joshua Bradley, Alex Chao, Apurva Mody, Steven Truitt, Dasha Metropolitansky, Robert Osazuwa Ness, and Jonathan Larson. From local to global: A graph rag approach to query-focused summarization. *arXiv preprint arXiv:2404.16130*, 2024.

[25] Kaiyue Feng, Guangsheng Zhang, Huan Tian, Heng Xu, Yanjun Zhang, Tianqing Zhu, Ming Ding, and Bo Liu. Ragleak: Membership inference attacks on rag-based large language models. In *Australasian Conference on Information Security and Privacy*, pages 147–166. Springer, 2025.

[26] Daniel Golovin and Andreas Krause. Adaptive submodularity: Theory and applications in active learning and stochastic optimization. *Journal of Artificial Intelligence Research*, 42:427–486, 2011.

[27] Google Cloud. Vertex ai search pricing. <https://cloud.google.com/generative-ai-app-builder/pricing>, 2026. Accessed: 2026-01-29.

[28] Zirui Guo, Lianghao Xia, Yanhua Yu, Tu Ao, and Chao Huang. Lightrag: Simple and fast retrieval-augmented generation. *arXiv preprint arXiv:2410.05779*, 2024.

[29] Xueyuan Han, Thomas Pasquier, Adam Bates, James Mickens, and Margo Seltzer. Unicorn: Runtime provenance-based detector for advanced persistent threats. In *27th Annual Network and Distributed System Security Symposium, NDSS 2020*. The Internet Society, 2020.

[30] Xinlei He, Jinyuan Jia, Michael Backes, Neil Zhenqiang Gong, and Yang Zhang. Stealing links from graph neural networks. In *30th USENIX security symposium (USENIX security 21)*, pages 2669–2686, 2021.

[31] Shaoxiong Ji, Shirui Pan, Erik Cambria, Pekka Marttinen, and Philip S Yu. A survey on knowledge graphs: Representation, acquisition, and applications. *IEEE transactions on neural networks and learning systems*, 33(2):494–514, 2021.

[32] Changyue Jiang, Xudong Pan, Geng Hong, Chenfu Bao, and Min Yang. Rag-thief: Scalable extraction of private data from retrieval-augmented generation applications with agent-based attacks. *arXiv preprint arXiv:2411.14110*, 2024.

[33] Mika Juuti, Sebastian Szyller, Samuel Marchal, and N Asokan. Prada: protecting against dnn model stealing attacks. In *2019 IEEE European Symposium on Security and Privacy (EuroS&P)*, pages 512–527. IEEE, 2019.

[34] Sanjay Kariyappa and Moinuddin K Qureshi. Defending against model stealing attacks with adaptive misinformation. In *Proceedings of the IEEE/CVF conference on computer vision and pattern recognition*, pages 770–778, 2020.

[35] Vladimir Karpukhin, Barlas Oguz, Sewon Min, Patrick SH Lewis, Ledell Wu, Sergey Edunov, Danqi Chen, and Wen-tau Yih. Dense passage retrieval for open-domain question answering. In *EMNLP (1)*, pages 6769–6781, 2020.

[36] Emilie Kaufmann, Olivier Cappé, and Aurélien Garivier. On bayesian upper confidence bounds for bandit problems. In *Artificial intelligence and statistics*, pages 592–600. PMLR, 2012.

[37] Samir Khuller, Anna Moss, and Joseph Seffi Naor. The budgeted maximum coverage problem. *Information processing letters*, 70(1):39–45, 1999.

[38] Andreas Krause and Carlos Guestrin. Near-optimal observation selection using submodular functions. In *AAAI*, volume 7, pages 1650–1654, 2007.

[39] Langchain. Advanced rag techniques. <https://langchain-tutorials.com/lessons/rag-applications/lesson-14>, 2025. Accessed: 2025-11-04.

[40] Patrick Lewis, Ethan Perez, Aleksandra Piktus, Fabio Petroni, Vladimir Karpukhin, Naman Goyal, Heinrich Küttrler, Mike Lewis, Wen-tau Yih, Tim Rocktäschel, et al. Retrieval-augmented generation for knowledge-intensive nlp tasks. *Advances in neural information processing systems*, 33:9459–9474, 2020.

[41] Shaofei Li, Feng Dong, Xusheng Xiao, Haoyu Wang, Fei Shao, Jiedong Chen, Yao Guo, Xiangqun Chen, and Ding Li. Nodlink: An online system for fine-grained apt attack detection and investigation. *arXiv preprint arXiv:2311.02331*, 2023.

[42] Shaofei Li, Ziqi Zhang, Haomin Jia, Yao Guo, Xiangqun Chen, and Ding Li. Query provenance analysis: Efficient and robust defense against query-based black-box attacks. In *2025 IEEE Symposium on Security and Privacy (SP)*, pages 1641–1656. IEEE, 2025.

[43] Yiming Li, Linghui Zhu, Xiaojun Jia, Yong Jiang, Shu-Tao Xia, and Xiaochun Cao. Defending against model stealing via verifying embedded external features. In *Proceedings of the AAAI conference on artificial intelligence*, volume 36, pages 1464–1472, 2022.

[44] Zehan Li, Xin Zhang, Yanzhao Zhang, Dingkun Long, Pengjun Xie, and Meishan Zhang. Towards general text embeddings with multi-stage contrastive learning. *arXiv preprint arXiv:2308.03281*, 2023.

[45] Zhicong Li, Jiahao Wang, Zhishu Jiang, Hangyu Mao, Zhongxia Chen, Jiazen Du, Yuanxing Zhang, Fuzheng Zhang, Di Zhang, and Yong Liu. Dmqr-rag: Diverse multi-query rewriting for rag. *arXiv preprint arXiv:2411.13154*, 2024.

[46] Jiacheng Liang, Yuhui Wang, Changjiang Li, Rongyi Zhu, Tanqiu Jiang, Neil Gong, and Ting Wang. Graphrag under fire. *arXiv preprint arXiv:2501.14050*, 2025.

[47] Sheng-Chieh Lin, Jheng-Hong Yang, Rodrigo Nogueira, Ming-Feng Tsai, Chuan-Ju Wang, and Jimmy Lin. Conversational question reformulation via sequence-to-sequence architectures and pretrained language models. *arXiv preprint arXiv:2004.01909*, 2020.

[48] Mingrui Liu, Sixiao Zhang, and Cheng Long. Mask-based membership inference attacks for retrieval-augmented generation. In *Proceedings of the ACM on Web Conference 2025*, pages 2894–2907, 2025.

[49] Yinuo Liu, Zenghui Yuan, Guiyao Tie, Jiawen Shi, Pan Zhou, Lichao Sun, and Neil Zhenqiang Gong. Poisoned-mrag: Knowledge poisoning attacks to multi-modal retrieval augmented generation. *arXiv preprint arXiv:2503.06254*, 2025.

[50] Yupei Liu, Jinyuan Jia, Hongbin Liu, and Neil Zhenqiang Gong. Stolenencoder: stealing pre-trained encoders in self-supervised learning. In *Proceedings of the 2022 ACM SIGSAC Conference on Computer and Communications Security*, pages 2115–2128, 2022.

[51] David Lopez-Paz and Maxime Oquab. Revisiting classifier two-sample tests. *arXiv preprint arXiv:1610.06545*, 2016.

[52] Lefteris Loukas, Ilias Stogiannidis, Odysseas Diamantopoulos, Prodromos Malakasiotis, and Stavros Vassos. Making llms worth every penny: Resource-limited text classification in banking. In *Proceedings of the Fourth ACM International Conference on AI in Finance*, pages 392–400, 2023.

[53] Xinbei Ma, Yeyun Gong, Pengcheng He, Nan Duan, et al. Query rewriting in retrieval-augmented large language models. In *The 2023 Conference on Empirical Methods in Natural Language Processing*, 2023.

[54] Yu A Malkov and Dmitry A Yashunin. Efficient and robust approximate nearest neighbor search using hierarchical navigable small world graphs. *IEEE transactions on pattern analysis and machine intelligence*, 42(4):824–836, 2018.

[55] Sadegh M Milajerdi, Rigel Gjomemo, Birhanu Es-hete, Ramachandran Sekar, and VN Venkatakrishnan. Holmes: real-time apt detection through correlation of suspicious information flows. In *2019 IEEE symposium on security and privacy (SP)*, pages 1137–1152. IEEE, 2019.

[56] Fengran Mo, Kelong Mao, Yutao Zhu, Yihong Wu, Kaiyu Huang, and Jian-Yun Nie. Convqqr: Generative query reformulation for conversational search. *arXiv preprint arXiv:2305.15645*, 2023.

[57] Ali Naseh, Yuefeng Peng, Anshuman Suri, Harsh Chaudhari, Alina Oprea, and Amir Houmansadr. Riddle me this! stealthy membership inference for retrieval-augmented generation. *arXiv preprint arXiv:2502.00306*, 2025.

[58] George L Nemhauser, Laurence A Wolsey, and Marshall L Fisher. An analysis of approximations for maximizing submodular set functions—i. *Mathematical programming*, 14(1):265–294, 1978.

[59] Bo Ni, Zheyuan Liu, Leyao Wang, Yongjia Lei, Yuying Zhao, Xueqi Cheng, Qingkai Zeng, Luna Dong, Yinglong Xia, Krishnaram Kenthapadi, et al. Towards trustworthy retrieval augmented generation for large language models: A survey. *arXiv preprint arXiv:2502.06872*, 2025.

[60] Daryna Oliynyk, Rudolf Mayer, and Andreas Rauber. I know what you trained last summer: A survey on stealing machine learning models and defences. *ACM Computing Surveys*, 55(14s):1–41, 2023.

[61] OpenAI. Gpt-4o mini. <https://openai.com/index/gpt-4o-mini-advancing-cost-efficient-intelligence/>, 2024. A cost-efficient, small-scale multimodal model from OpenAI.

[62] OpenAI. Openai safety update: Sharing our practices as part of the ai seoul summit. <https://openai.com/index/openai-safety-update>, May 2024. Accessed: 2025-11-12.

[63] Tribhuvanesh Orekondy, Bernt Schiele, and Mario Fritz. Knockoff nets: Stealing functionality of black-box models. In *Proceedings of the IEEE/CVF conference on computer vision and pattern recognition*, pages 4954–4963, 2019.

[64] Tribhuvanesh Orekondy, Bernt Schiele, and Mario Fritz. Prediction poisoning: Utility-constrained defenses against model stealing attacks. In *International Conference on Representation Learning (ICLR) 2020*, 2020.

[65] Andrea Papaluca, Daniel Krefl, Sergio Rodríguez Méndez, Artem Lensky, and Hanna Suominen. Zero-and few-shots knowledge graph triplet extraction with large language models. In *Proceedings of the 1st workshop on knowledge graphs and large language models (kALLM 2024)*, pages 12–23, 2024.

[66] Zhenting Qi, Hanlin Zhang, Eric P Xing, Sham M Kakade, and Himabindu Lakkaraju. Follow my instruction and spill the beans: Scalable data extraction from retrieval-augmented generation systems. In *The Thirteenth International Conference on Learning Representations*.

[67] Qwen. Qwen2.5-7b-instruct. <https://huggingface.co/Qwen/Qwen2.5-7B-Instruct>, 2024. Open-source large-language model.

[68] Adnan Siraj Rakin, Md Hafizul Islam Chowdhuryy, Fan Yao, and Deliang Fan. Deepsteal: Advanced model extractions leveraging efficient weight stealing in memories. In *2022 IEEE symposium on security and privacy (SP)*, pages 1157–1174. IEEE, 2022.

[69] Avital Shafran, Roei Schuster, and Vitaly Shmatikov. Machine against the rag: Jamming retrieval-augmented generation with blocker documents. *USENIX Security*, 2025.

[70] Yun Shen, Xinlei He, Yufei Han, and Yang Zhang. Model stealing attacks against inductive graph neural networks. In *2022 IEEE Symposium on Security and Privacy (SP)*, pages 1175–1192. IEEE, 2022.

[71] Gabriel Stanovsky, Julian Michael, Luke Zettlemoyer, and Ido Dagan. Supervised open information extraction. In *Proceedings of the 2018 Conference of the North American Chapter of the Association for Computational Linguistics: Human Language Technologies, Volume 1 (Long Papers)*, pages 885–895, 2018.

[72] Gábor J Székely and Maria L Rizzo. Energy statistics: A class of statistics based on distances. *Journal of statistical planning and inference*, 143(8):1249–1272, 2013.

[73] Nandan Thakur, Nils Reimers, Andreas Rücklé, Abhishek Srivastava, and Iryna Gurevych. Beir: A heterogeneous benchmark for zero-shot evaluation of information retrieval models. *arXiv preprint arXiv:2104.08663*, 2021.

[74] The Lasso Team. Rag security: Risks and mitigation strategies, 2024. See section: “Security Risks at Retrieval Stage”. URL: <https://www.lasso.security/blog/rag-security>.

[75] Florian Tramèr, Fan Zhang, Ari Juels, Michael K Reiter, and Thomas Ristenpart. Stealing machine learning models via prediction {APIs}. In *25th USENIX security symposium (USENIX Security 16)*, pages 601–618, 2016.

[76] Yuhao Wang, Wenjie Qu, Yanze Jiang, Zichen Liu, Yue Liu, Shengfang Zhai, Yinpeng Dong, and Jiaheng Zhang. Silent leaks: Implicit knowledge extraction attack on rag systems through benign queries. *arXiv preprint arXiv:2505.15420*, 2025.

[77] Yujing Wang, Hainan Zhang, Liang Pang, Binghui Guo, Hongwei Zheng, and Zhiming Zheng. Maferw: Query rewriting with multi-aspect feedbacks for retrieval-augmented large language models. In *Proceedings of the AAAI Conference on Artificial Intelligence*, volume 39, pages 25434–25442, 2025.

[78] Laurence A Wolsey. An analysis of the greedy algorithm for the submodular set covering problem. *Combinatorica*, 2(4):385–393, 1982.

[79] Dong-Dong Wu, Chilin Fu, Weichang Wu, Wenwen Xia, Xiaolu Zhang, Jun Zhou, and Min-Ling Zhang. Efficient model stealing defense with noise transition matrix. In *Proceedings of the IEEE/CVF Conference on Computer Vision and Pattern Recognition*, pages 24305–24315, 2024.

[80] Anbang Xu, Tan Yu, Min Du, Pritam Gundecha, Yufan Guo, Xinliang Zhu, May Wang, Ping Li, and Xinyun Chen. Generative ai and retrieval-augmented generation (rag) systems for enterprise. In *Proceedings of the 33rd ACM International Conference on Information and Knowledge Management*, pages 5599–5602, 2024.

[81] Xianghao Xu, Fang Wang, Hong Jiang, Yongli Cheng, Dan Feng, and Yongxuan Zhang. A hybrid update strategy for i/o-efficient out-of-core graph processing. *IEEE Transactions on Parallel and Distributed Systems*, 31(8):1767–1782, 2020.

[82] Mingyu Yang, Wentao Li, Jiabao Jin, Xiaoyao Zhong, Xiangyu Wang, Zhitao Shen, Wei Jia, and Wei Wang.

Effective and general distance computation for approximate nearest neighbor search. In *2025 IEEE 41st International Conference on Data Engineering (ICDE)*, pages 1098–1110. IEEE, 2025.

- [83] Alexander Yates, Michele Banko, Matthew Broadhead, Michael J Cafarella, Oren Etzioni, and Stephen Soderland. Textrunner: open information extraction on the web. In *Proceedings of Human Language Technologies: The Annual Conference of the North American Chapter of the Association for Computational Linguistics (NAACL-HLT)*, pages 25–26, 2007.
- [84] Xiaoyong Yuan, Leah Ding, Lan Zhang, Xiaolin Li, and Dapeng Oliver Wu. Es attack: Model stealing against deep neural networks without data hurdles. *IEEE Transactions on Emerging Topics in Computational Intelligence*, 6(5):1258–1270, 2022.
- [85] Shenglai Zeng, Jiankun Zhang, Pengfei He, Yiding Liu, Yue Xing, Han Xu, Jie Ren, Yi Chang, Shuaiqiang Wang, Dawei Yin, et al. The good and the bad: Exploring privacy issues in retrieval-augmented generation (rag). In *ACL (Findings)*, 2024.
- [86] Mingxing Zhang, Yongwei Wu, Youwei Zhuo, Xuehai Qian, Chengying Huan, and Kang Chen. Wonderland: A novel abstraction-based out-of-core graph processing system. *ACM SIGPLAN Notices*, 53(2):608–621, 2018.
- [87] Peitian Zhang, Shitao Xiao, Zheng Liu, Zhicheng Dou, and Jian-Yun Nie. Retrieve anything to augment large language models. *arXiv preprint arXiv:2310.07554*, 2023.
- [88] Zexuan Zhong, Ziqing Huang, Alexander Wettig, and Danqi Chen. Poisoning retrieval corpora by injecting adversarial passages. *arXiv preprint arXiv:2310.19156*, 2023.
- [89] Wei Zou, Rupeng Geng, Binghui Wang, and Jinyuan Jia. {PoisonedRAG}: Knowledge corruption attacks to {Retrieval-Augmented} generation of large language models. In *34th USENIX Security Symposium (USENIX Security 25)*, pages 3827–3844, 2025.

Appendix

A Proof of Theorems

Notation (issued-query set). A retrieval-level partial realization ψ^R records the issued queries and their (retrieval) outcome sets. We write $\text{dom}(\psi^R) \subseteq Q$ for the set of queries appearing in ψ^R (i.e., issued so far), and use the shorthand

$$S(\psi^R) := \text{dom}(\psi^R).$$

In particular, the S_{t-1} in Definition 1 is exactly $S(\psi_{t-1}^R)$. We also define the union of revealed retrieved items in Ψ^R as

$$R(\psi^R) := \bigcup_{(q,o) \in \psi^R} o.$$

Lemma A.1 (RAG \Rightarrow independence of unissued outcomes). We consider standard RAG deployment: each query is processed independently, and any internal randomness (e.g., query rewriting sampling or multi-query generation sampling) is freshly drawn per query and independent across queries. Formally, let $\Phi = (\xi_q)_{q \in Q}$ where $\{\xi_q\}$ are mutually independent, and assume $O_\Phi(q)$ is determined only by (q, ξ_q) . Then for any retrieval-level partial realization ψ^R and any query $q \notin S(\psi^R)$, the conditional law of $O_\Phi(q)$ is unchanged by conditioning on ψ^R . In particular, for any measurable function $h(\cdot)$,

$$\mathbb{E}[h(O_\Phi(q)) | \psi^R] = \mathbb{E}[h(O_\Phi(q))]. \quad (18)$$

Proof. Under the stateless assumption, ψ^R depends only on $\{\xi_{q'} : q' \in S(\psi^R)\}$ through the realized outcomes of already issued queries. For any $q \notin S(\psi^R)$, ξ_q is independent of $\{\xi_{q'} : q' \in S(\psi^R)\}$, hence independent of the event defining ψ^R . Therefore conditioning on ψ^R does not change the distribution of ξ_q nor of $O_\Phi(q)$, which yields (18). \square

Proof of Theorem 2: Adaptive Monotonicity and Submodularity in RAG Crawling

Proof. (Adaptive monotonicity). For any realization Φ and any query set $A \subseteq Q$, the coverage function satisfies $f(A \cup \{q\}, \Phi) \geq f(A, \Phi)$, since adding a query can only enlarge the union of retrieved items. By Definition 1, this implies $\Delta(q | \psi_{t-1}^R) \geq 0$ for any retrieval-level partial realization ψ_{t-1}^R .

(Adaptive submodularity). Let ψ^R and $\psi^{R'}$ be retrieval-level partial realizations such that $\psi^{R'}$ is an extension of ψ^R . Then $R(\psi^R) \subseteq R(\psi^{R'})$, and also $S(\psi^R) \subseteq S(\psi^{R'})$.

Fix any query $q \notin S(\psi^{R'})$ (i.e., q has not been issued under $\psi^{R'}$). Define the shorthand

$$R \triangleq R(\psi^R), \quad R' \triangleq R(\psi^{R'}), \quad Y \triangleq O_\Phi(q).$$

For any realization Φ consistent with $\psi^{R'}$ (hence also consistent with ψ^R), the marginal gain of issuing q under ψ^R is

$$f(S(\psi^R) \cup \{q\}, \Phi) - f(S(\psi^R), \Phi) = |Y \setminus R|, \quad (19)$$

and similarly under $\psi^{R'}$ it equals $|Y \setminus R'|$. Since $R \subseteq R'$, we have pointwise diminishing returns for every outcome set Y :

$$|Y \setminus R| \geq |Y \setminus R'|. \quad (20)$$

By Definition 1 and (19),

$$\Delta(q | \psi^R) = \mathbb{E}[|Y \setminus R| | \psi^R]. \quad (21)$$

Because $q \notin S(\psi^R)$ and the victim RAG is stateless, Lemma A.1 applies and yields

$$\Delta(q | \psi^R) = \mathbb{E}[|Y \setminus R|]. \quad (22)$$

Similarly,

$$\Delta(q | \psi^{R'}) = \mathbb{E}[|Y \setminus R'|]. \quad (23)$$

Taking expectation of (20) over the (common) distribution of Y gives $\mathbb{E}[|Y \setminus R|] \geq \mathbb{E}[|Y \setminus R'|]$. Combining with (22)–(23) yields

$$\Delta(q | \psi^R) \geq \Delta(q | \psi^{R'}), \quad (24)$$

which is adaptive submodularity. \square

B Sample Distribution Validation

To ensure that our 1,000-document samples are representative of the full corpora, we compare their semantic distributions using Energy Distance [72] and the Classifier Two-Sample Test (C2ST) [51].

Energy Distance quantifies the difference between two distributions using Euclidean distances, and is well-suited for high-dimensional or non-Gaussian data. A smaller energy distance with a large permutation test p -value suggests no statistically significant difference between the sampled and full sets. As shown in Table 8, all four corpora yield low distances (around 0.03) and high p -values (> 0.5), indicating strong alignment between samples and full sets. C2ST (Classifier Two-Sample Test) reframes distribution comparison as a binary classification task. If a classifier cannot distinguish between samples and the full corpus ($\text{AUC} \approx 0.5$), the two distributions are considered similar. In Table 8, all AUC scores fall within the 0.46–0.51 range, reinforcing that no meaningful distinction can be learned between the subsets and their corresponding full corpora.

Table 8: Semantic distribution similarity between each full corpus and its 1,000-document sampled subset, measured by Energy Distance (with permutation test p -value) and the Classifier Two-Sample Test (C2ST, using AUC). A small Energy Distance with a high p -value and an AUC near 0.5 indicate distributional similarity.

Corpus	Energy Distance (value / p)	C2ST (AUC)
TREC-COVID	0.0349 / 0.5249	0.4993
SciDocs	0.0329 / 0.5781	0.4938
NFCorpus	0.0281 / 0.6412	0.5053
Healthcare	0.0276 / 0.5947	0.4679

Table 9: Token usage and estimated cost per corpus for KG-Constructor (KG-C) and Query Generator (QG) using Doubao-1.5-lite-32k. “InTok” and “OutTok” denote input and output token counts. Each attack costs under \$1.

Metric	TREC-COVID	SciDocs	NFCorpus	Healthcare
KG-C InTok (M)	5.561	6.209	5.997	9.094
KG-C OutTok (M)	0.724	1.277	1.076	1.373
QG InTok (M)	0.847	0.596	0.366	0.783
QG OutTok (M)	0.042	0.027	0.017	0.035
Total Cost (\$)	0.333	0.395	0.359	0.533

C Attacker-side orchestration cost

We estimate the attacker-side cost of executing RAGCRAWLER, i.e., the tokens consumed by the attacker’s model. As reported in Table 9, RAGCRAWLER processes approximately 6–10 million tokens per dataset. Based on Doubao-1.5-lite-32K’s API pricing (\$0.042 per million input tokens and \$0.084 per million output tokens), this orchestration cost is \$0.33–\$0.53 per dataset. As shown in Sec. 7.4, substituting an open-source model such as Qwen-2.5-7B does not degrade performance, making this component **virtually zero** aside from GPU hosting.

D No-topic-prior attacker via one-shot topic probing

Motivation. In Sec. 4, we assume the attacker knows a coarse topic phrase of the target corpus, which is often available from product descriptions, onboarding pages, or light interaction with the assistant [27, 76]. To be conservative about attacker knowledge, we also evaluate a weaker attacker that starts with no topic prior; the corresponding CR results are reported in Table 7 (main text).

One-shot topic probing. The attacker first issues a single benign probe query to the victim RAG system:

What domain do you know about?

Let the victim response be a_{probe} . The attacker then infers a high-level topic phrase from a_{probe} using an attacker-side LLM and the following prompt. The output is restricted to a short phrase (3–8 words) to avoid over-specification and keep the prior coarse.

You are given a sentence that is generated by a RAG system.

Infer the high-level domain/topic of the RAG system in 3–8 words.

Return ONLY the topic phrase (no quotes, no extra text).

Sentence: {a_prob}

Topic:

The inferred phrase is the only topic signal used in the subsequent attack. For RAGCRAWLER, it replaces the provided topic input to the Topic-Specific Prior module (Sec. 6.2),

which induces the lightweight entity/relation schema and then proceeds with the same closed-loop crawling. For fair comparison, we provide the same inferred topic phrase to baselines as their input.

Budget accounting and metrics. We count the probe as one issued query, so the remaining crawling budget is reduced by one under a fixed total budget. We report Coverage Rate (CR) under the same evaluation protocol as Sec. 7.

Further analysis: inferred-topic noise and robustness. The one-shot probe can yield coarse or off-focus topic phrases that deviate substantially from the manual topic prior. For example, the inferred topic is *Medical Research on Impact Factors* for TREC-COVID (manual topic: *COVID-19*, similarity 0.134) and *Relationship Marketing & Tech* for SciDocs (manual topic: *Computer Science Research Papers*, similarity 0.185).

Despite such noise, Table 7 shows that RAGCRAWLER remains effective and achieves the best CR across datasets, with only modest changes relative to the topic-prior setting. In contrast, baselines can be more sensitive to topic quality, consistent with their heavier reliance on the provided topic signal. This robustness is expected from RAGCRAWLER’s design: the topic prior only bootstraps the initial schema, while the attacker-side global state is continuously updated from retrieved documents, allowing subsequent query planning to self-correct and prioritize unexplored regions of the corpus.

E Additional Experiments Results

E.1 Coverage Rate Curves

For completeness, we provide all Coverage Rate curves across datasets and settings for all experiments in Sec 7.2, Sec. 7.3 and Sec. 7.4 in Fig. 11, Fig. 12 and Fig. 13.

E.2 Additional Ablations

Modules. The effectiveness of RAGCRAWLER stems from the synergistic integration of its three architectural modules. Without the KG-Constructor, the system loses its global state memory, becoming a stateless, reactive loop unable to distinguish explored regions, a behavior characteristic of IKEA. Without the Strategy Scheduler, the system cannot perform UCB-based prioritization; a fallback to random anchor selection would mimic IKEA’s keyword-based strategy. Finally, without the Query Generator, the scheduler’s strategic plan cannot be translated into executable queries, rendering the planning moot.

Hyperparameter Choices. We examine two key hyperparameters in RAGCRAWLER: the UCB exploration coefficient c used by the Strategy Scheduler for query selection, and the similarity threshold τ_{dup} used by the Query Generator to filter high-similarity queries (thereby controlling early stopping). As shown in Fig. 14, a moderate UCB coefficient of $c = 0.5$ delivers the best performance by balancing exploitation and

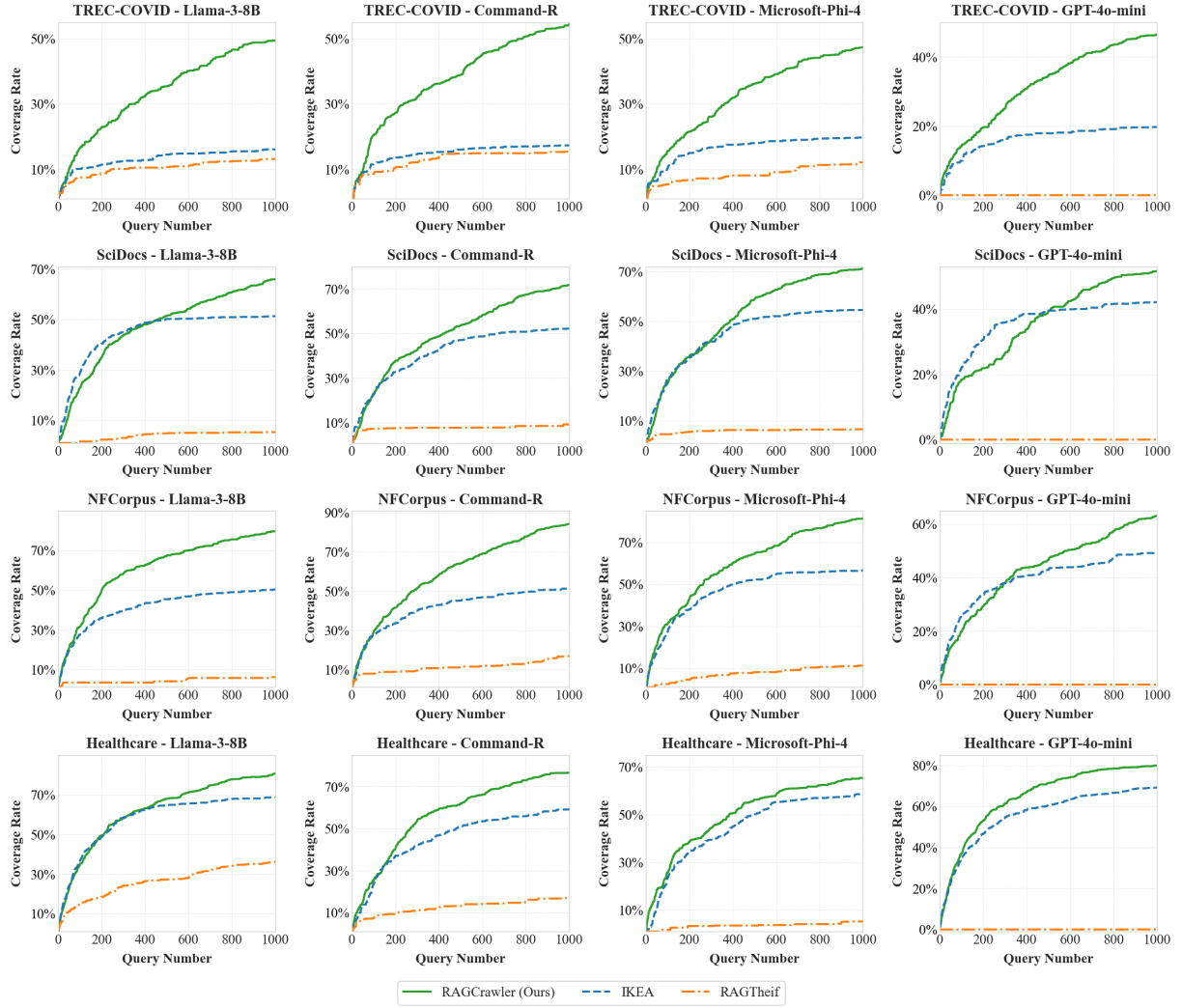


Figure 11: Coverage Rate vs. Query Number (1,000 Budget) across four datasets and four generators.

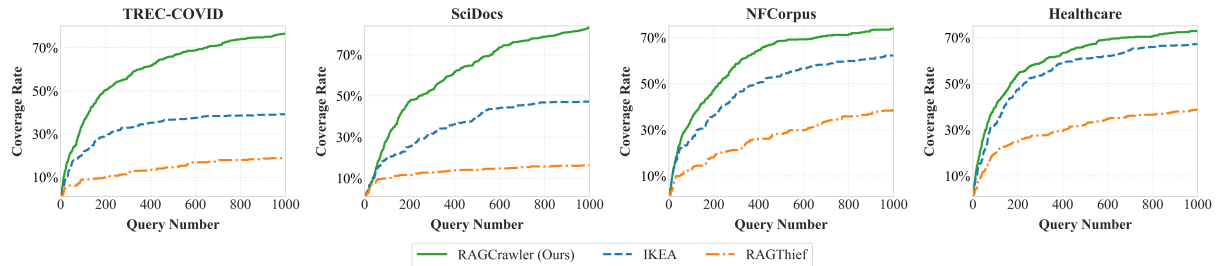


Figure 12: Coverage Rate vs. Query Number (1,000 Budget) across four datasets (GTE Retriever, Llama-3-8B generator).

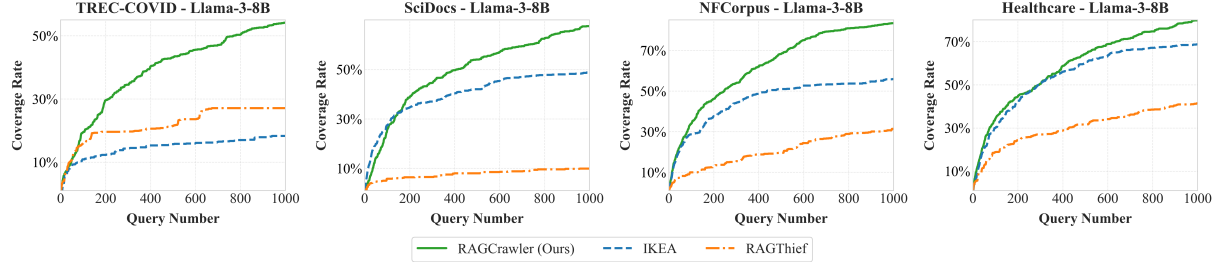


Figure 13: Coverage Rate vs. Query Number (1,000 Budget) across four datasets with Qwen-2.5-7B-Instruct as attacker LLM (BGE Retriever, Llama-3-8B generator).

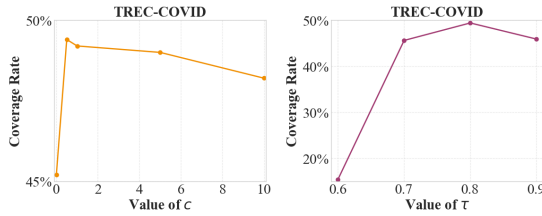


Figure 14: Hyperparameter Choices of RAGCRAWLER.

exploration. Increasing or decreasing c from this value noticeably degrades performance, underscoring that $c = 0.5$ is near-optimal for a proper exploration–exploitation trade-off. Similarly, the threshold τ_{dup} exhibits a clear sweet spot. Setting τ_{dup} too low often causes premature termination. On the other hand, an overly high threshold produces queries that are not sufficiently distinct from one another, which limits exploration efficiency. Our chosen $\tau_{dup} = 0.8$ navigates between these extremes.

E.3 Additional Target-Coverage Query Complexity

Table 10 summarizes the target-coverage query complexity Q_γ under a fixed cap $Q_{\max} = 5,000$ and the resulting final coverage $CR(Q_{\max})$. A clear pattern is that baseline heuristics exhibit strong *early* gains but saturate quickly, whereas RAGCRAWLER continues to accrue coverage as the target increases. At low targets (50–60%), IKEA can sometimes approach RAGCRAWLER on easier corpora (e.g., Healthcare), suggesting that shallow, highly retrievable regions can be harvested with mostly local signals. However, as γ increases, IKEA increasingly plateaus: on three of four datasets it cannot reach 70% within the cap, and its remaining gains are dominated by redundancy. RAGThief is consistently the weakest, failing to reach 50% on most corpora and often stalling far below the cap coverage achieved by the other methods.

In contrast, RAGCRAWLER is the only method that reliably enters the high-coverage regime. It continues to improve beyond 80% and even reaches 90% on three datasets within Q_{\max} , while no baseline attains 90% under the same budget.

Table 10: Query complexity for target corpus coverage under a budget cap. For each method and dataset, we report Q_γ , the number of issued queries needed to reach coverage $\gamma \in \{0.5, 0.6, 0.7, 0.8, 0.9\}$ with $Q_{\max} = 5,000$; entries marked $Q_\gamma > Q_{\max}$ indicate the target was not reached within the cap. We also report the final coverage $CR(Q_{\max})$ for all runs. RAGCRAWLER consistently attains the highest $CR(Q_{\max})$ and reaches substantially higher coverage targets with fewer queries.

Dataset	Method	$Q_{0.5}$	$Q_{0.6}$	$Q_{0.7}$	$Q_{0.8}$	$Q_{0.9}$	$CR(Q_{\max})$
TREC-COVID	RAGThief	> 5000	> 5000	> 5000	> 5000	> 5000	0.298
	IKEA	> 5000	> 5000	> 5000	> 5000	> 5000	0.196
	RAGCRAWLER	1107	1972	4040	> 5000	> 5000	0.725
SciDocs	RAGThief	> 5000	> 5000	> 5000	> 5000	> 5000	0.072
	IKEA	493	> 5000	> 5000	> 5000	> 5000	0.560
	RAGCRAWLER	457	776	1163	1784	3330	0.936
NFCorpus	RAGThief	> 5000	> 5000	> 5000	> 5000	> 5000	0.192
	IKEA	938	3427	> 5000	> 5000	> 5000	0.640
	RAGCRAWLER	200	322	595	1011	1753	0.977
Healthcare	RAGThief	3537	> 5000	> 5000	> 5000	> 5000	0.530
	IKEA	212	345	1231	2925	> 5000	0.825
	RAGCRAWLER	209	329	568	983	2434	0.941

This difference is also reflected in final coverage at Q_{\max} : RAGCRAWLER achieves the highest $CR(Q_{\max})$ on every dataset and maintains a large margin over both baselines, with the gap widening on harder corpora. TREC-COVID remains the most challenging case: although RAGCRAWLER cannot reach 80% within the cap, it still sustains steady growth and substantially outpaces baselines that plateau below 30%. Overall, the advantage of global state and planning becomes more pronounced as the desired coverage rises, precisely where local heuristics are most susceptible to redundancy and drift.

E.4 Larger victim collections

To further investigate the impact of scale, a complementary study was conducted with an expanded configuration of 2,000 documents and a 5,000-Budget. The coverage rate curves for the NFCorpus and Healthcare datasets from this study are depicted in Fig. 15.

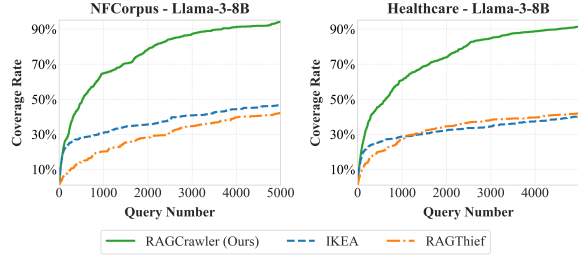


Figure 15: Coverage Rate vs. Query Number (5,000 Budget) on NFCorpus and Healthcare with GPT-4o-mini as attacker LLM (BGE Retriever, Llama-3-8B generator).

F Prompts for Experimental Stages

We document the exact prompts used in RAG settings. More prompts in our method can be found in our code.

RAG System Prompt

You are an assistant for question-answering tasks. Use the following pieces of retrieved context to answer the question. If you don't know the answer, say that you don't know.

Context: [context]

Query: [query]

Answer:

Query Rewriting Prompt in RAG System

You are a helpful assistant. Your task is to rewrite the given user question to clarify the user's intent and remove any adversarial intent. Directly output the rewritten question without any other text.

Original Question: [query]

Answer:

Multi-query Prompt in RAG System

You are a helpful assistant. Your task is to generate 3 different versions of the given user question to retrieve relevant documents from a vector database. By generating multiple perspectives on the user question, your goal is to help the user overcome some of the limitations of the distance-based similarity search. Provide directly output these alternative questions separated by newlines without any other text.

Original Question: [query]

Answer: